# CHAPTER 4

# RESULTS AND DISCUSSION - COAL ANALYSIS

In this chapter, the results obtained from the detailed characterisation of coals from mines in the Highveld coalfield as well as the feed coal are discussed as the basis for a better understanding of the mineralogical and chemical properties of the individual components in the feedstocks used for coal conversion processes.

## 4.1 Chemical analyses of coals from six different Highveld coal mines and feed coal to the coal conversion process

### 4.1.1 Proximate analysis

Proximate analysis data (Table 4.1) show that the samples yield 30-34% volatile matter on a dry ash free (daf) basis. The inherent moisture content of the coals ranged between 2.9% and 3.8% and the total sulphur content from 0.7% to 1.1%. The ash yield of the samples tested (air-dried basis) ranged between 22.1% and 29.7%.

**Table 4.1:** Proximate analyses (air dried basis) of the coals tested

| Mine Number | 1 | 2 | 3 | 4 | 5 | 6 |
|---|---|---|---|---|---|---|
| Moisture (%) | 3.30 | 2.90 | 3.20 | 3.40 | 3.00 | 3.80 |
| Ash (%) | 24.50 | 29.00 | 29.70 | 27.20 | 26.80 | 22.10 |
| Volatile matter (%) | 21.70 | 22.90 | 21.30 | 21.50 | 22.40 | 23.10 |
| Fixed carbon (%) | 50.50 | 45.20 | 45.80 | 47.90 | 47.80 | 51.00 |
| Total sulphur (%) | 1.10 | 1.00 | 0.80 | 1.00 | 1.10 | 0.70 |
| Volatile matter (daf basis, %) | 30.10 | 33.60 | 31.70 | 31.00 | 31.90 | 31.20 |

### 4.1.2 Ultimate analysis

Ultimate analysis data (Table 4.2) indicate that the coals contain high proportions of carbon (ranging from 77 - 80% daf), with relatively low concentrations of sulphur (0.9%-1.6% daf), nitrogen (2-2.2% daf) and hydrogen (ranging from 4-4.6% daf). The oxygen content of the coals (daf basis) was found by calculation to range from 12-16%.

**Table 4.2:** Normalised ultimate analyses of the coals tested (dry, ash-free basis)

| **Mine Number** | **1** | **2** | **3** | **4** | **5** | **6** |
|---|---|---|---|---|---|---|
| Carbon (%) | 79.90 | 78.50 | 77.10 | 77.80 | 79.00 | 77.90 |
| Hydrogen (%) | 4.36 | 4.55 | 4.07 | 4.12 | 4.59 | 4.29 |
| Nitrogen (%) | 2.12 | 2.00 | 1.97 | 2.00 | 2.08 | 2.00 |
| Total sulphur (%) | 1.55 | 1.41 | 1.15 | 1.50 | 1.62 | 0.92 |
| Oxygen (% by difference) | 12.10 | 13.50 | 15.7 | 14.60 | 12.70 | 14.90 |

### 4.1.3 XRF analysis

The normalised proportions of inorganic elements in the coal samples, derived from XRF analysis of the whole-coal samples, are given in Table 4.3. The XRF technique used is regarded as only semi-quantitative for sulphur, hence the sulphur contents are not reported. The results given in Table 4.3 also indicate that there are some variations in the chemical composition of the coal used in the study. These differences in compositions are attributed to the particle size of the coarse coal samples, which ranged from 13.2mm to 2.36mm, possibly producing heterogeneity that affected the sampling process.

The XRF analysis of the feed coal sample to gasification indicated that this sample contains 52.2% $SiO_2$, 26.2% $Al_2O_3$, 4.0% $Fe_2O_3$, 1.5% $TiO_2$, 0.7% $P_2O_5$, 8.1% CaO, 3.7% MgO, 0.7% $Na_2O$, 1.1%$K_2O$ and 1.9% S (normalised XRF results, excluding carbon and volatiles).

**Table 4.3**: Inorganic oxide percentages (wt %) from normalised XRF analysis of whole-coal samples

| Mine Number | 1 | 2 | 3 | 4 | 5 | 6 |
|---|---|---|---|---|---|---|
| $SiO_2$ | 57.16 | 55.38 | 55.91 | 52.20 | 57.43 | 55.68 |
| $Al_2O_3$ | 24.96 | 30.21 | 27.78 | 29.40 | 26.70 | 25.31 |
| $Fe_2O_3$ | 5.13 | 2.34 | 1.88 | 2.42 | 3.58 | 2.59 |
| $TiO_2$ | 1.21 | 1.26 | 1.42 | 1.64 | 1.17 | 1.33 |
| $P_2O_5$ | 0.32 | 0.76 | 0.53 | 0.86 | 0.89 | 0.68 |
| CaO | 7.49 | 6.54 | 8.26 | 9.27 | 7.03 | 10.60 |
| MgO | 1.67 | 1.42 | 2.02 | 1.84 | 1.23 | 2.06 |
| $Na_2O$ | 0.89 | 0.76 | 1.06 | 1.07 | 0.85 | 1.06 |
| $K_2O$ | 0.85 | 0.95 | 1.02 | 1.29 | 1.13 | 0.54 |

## 4.2 Petrographic analysis of coals from different Highveld coal mines

Petrographic analysis (Table 4.4) indicates that coals characterised in this study are inertinite-rich, with 64-77% inertinite and 19-30% vitrinite components on a mineral-free basis. It is clear from the results given in Table 4.4 that mines 5 and 6 contain slightly higher proportions of vitrinite and liptinite and lesser proportions of inertinite than the other coal samples analysed. The results from this table also show that the coals have a mean maximum vitrinite reflectance, measured on telocollinite, of around 0.70-0.75%. According to ISO 11760, the coals can be classified as medium-rank C bituminous coals.

**Table 4.4**: Petrographic analysis of coal samples from the different mines (vol. %, mineral free)

| Maceral Group | 1 | 2 | 3 | 4 | 5 | 6 |
|---|---|---|---|---|---|---|
| Vitrinite (%) | 19.2 | 25.8 | 20.5 | 20.6 | 31.6 | 27.1 |
| Liptinite (%) | 3.5 | 3.7 | 3.2 | 3.4 | 5.4 | 5.4 |
| Inertinite (%) | 77.3 | 70.6 | 76.3 | 76.1 | 64.0 | 67.5 |
| $Rv_{max}$ (%) | 0.72 | 0.70 | 0.75 | 0.72 | 0.70 | 0.70 |

## 4.3 Mineralogical analyses of LTA of coals from the different mines and feed coal

### 4.3.1 Mineralogy of LTA residues

Table 4.5 summarises the percentages of the individual minerals in each LTA of coals produced from the different coal mines, based on the powder XRD and SIROQUANT evaluation. Figures 4.1 and 4.2 illustrate the X-ray diffractograms of the LTA from each coal sample.

The results shown in Table 4.5 indicate that the coal sample from mine 4 contains a slightly lower proportion of mineral matter in comparison with the other coal samples analysed. The proportions of low-temperature (oxygen-plasma) ash in the coal samples were found to be 24.60-43.90 wt%, compared to the (high-temperature) ash yields of 22.10-29.70wt%, as determined by proximate analysis. The difference is largely because many of the minerals (kaolinite, calcite, dolomite, pyrite, siderite and illite) in the coal samples decompose at the high temperatures associated with ashing in proximate analysis, but remain stable under plasma-ashing conditions (Tables 4.1 and 4.5).

As indicated in Table 4.5 and Figures 4.2-4.3, the LTA derived from the six coals was made up mainly of kaolinite (44-51%), with a lesser proportion of quartz (15-22%), mica (4.5-7.4%) and dolomite (6.4-15%) and minor proportions of siderite ($FeCO_3$), calcite ($CaCO_3$), pyrite ($FeS_2$), anatase ($TiO_2$), and the aluminophosphate mineral, goyazite ($SrAl_3(PO_4)_2(OH)_5.H_2O$). It is interesting to note that the LTA of samples 1 and 6 contain no illite ($K_{1.5}Al_4(Si_{6.5}Al_{1.5})O_{20}(OH)_4$), whilst the LTA of coal samples from mines 2, 3, 4 and 5 contain admixed illite, ranging in abundance from 2 to 5.7%. A small proportion of bassanite ($CaSO_4.½H_2O$), which was probably derived from interaction of the organically-associated calcium in the coals with organic sulphur during the low-temperature ashing process, was also noted in the LTA samples of coals.

Further results on the clay fractions, based on the separate oriented aggregate XRD study, are provided in Table 4.6. The results differ from those given in Table 4.5, because only the smallest (<2 micron) particles were analysed for the results in Table 4.6. The nature of the sub-micron clay minerals (illite, smectite ($Na_{0.33}(Al_{1.67}Mg_{0.33})Si_4O_{10}(OH)_2$),

illite/smectite and kaolinite) may possibly be significant in clinker formation, as well as in the volatilisation of minor amounts of Al and Si during coal conversion processes.

**Table 4.5:** Mineralogical analyses of LTA from coal samples from the different mines (wt %)

| **Mine** | **1** | **2** | **3** | **4** | **5** | **6** |
|---|---|---|---|---|---|---|
| LTA | 31.90 | 43.90 | 33.60 | 24.60 | 36.20 | 34.50 |
| Quartz | 17.60 | 21.50 | 20.10 | 18.30 | 15.20 | 20.60 |
| Kaolinite | 51.40 | 50.40 | 50.80 | 47.60 | 44.00 | 49.50 |
| Illite | nd | 5.70 | 5.30 | 2.20 | 5.70 | nd |
| Mica | 10.40 | 7.40 | 4.50 | 4.50 | 6.90 | 7.00 |
| Calcite | 2.10 | 1.20 | 1.80 | 4.60 | 9.80 | 2.70 |
| Dolomite | 10.30 | 6.40 | 10.20 | 15.20 | 10.00 | 11.70 |
| Siderite | 0.00 | 1.30 | 0.30 | 1.40 | 0.40 | 0.90 |
| Pyrite | 2.40 | 1.40 | 2.60 | 2.00 | 1.40 | 1.60 |
| Bassanite | 2.10 | 1.40 | 1.90 | 2.50 | 2.50 | 1.60 |
| Goyazite | 1.00 | 1.70 | 1.40 | 0.90 | 3.00 | 2.70 |
| Anatase | 2.70 | 1.50 | 1.00 | 0.80 | 1.00 | 1.60 |

**Note**: nd: not detected.

The chemical composition of the coal ash expected in each of the coals was calculated from the mineral percentages listed in Table 4.5 and the chemical composition of the individual minerals based either on stoichiometry or on typical analyses of the same minerals published in the literature. The results (Table 4.7), normalised to exclude sulphur (as $SO_3$), are very similar to the data obtained from direct XRF analysis of the same coals, also normalised to a sulphur-free basis, presented in Table 4.3. Only minor differences are present in most cases, probably reflecting differences in the actual samples analysed in each instance, differences between stoichiometric and actual mineral compositions, as well as errors inherently associated with the two different techniques.

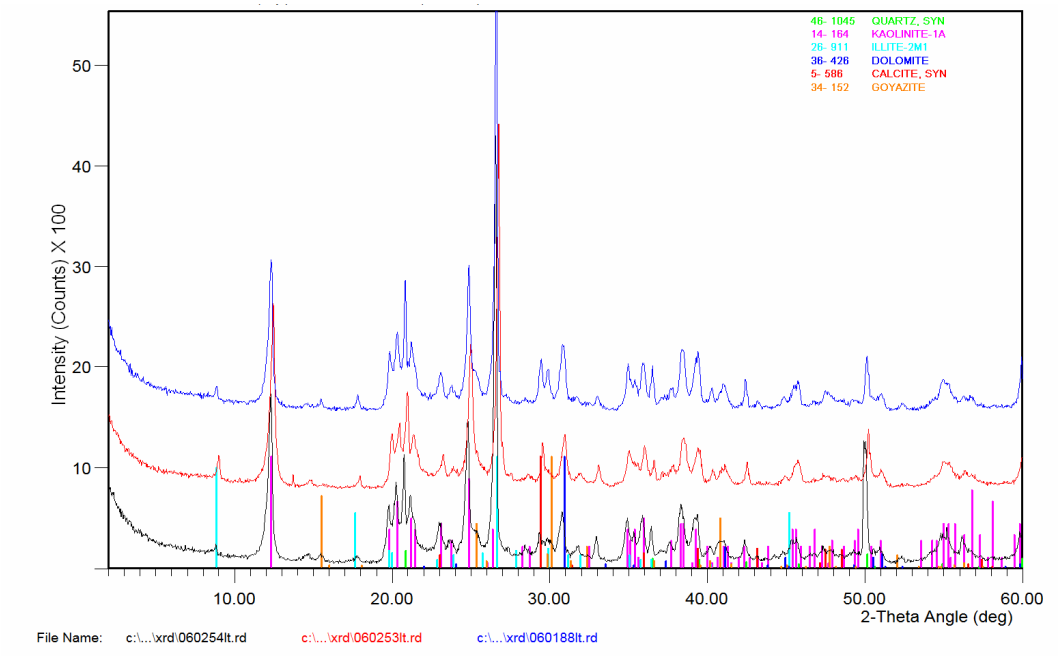


**Figure 4.1**: X-ray diffractograms of LTA from samples from mines 3 (top), 1 and 5 (bottom).

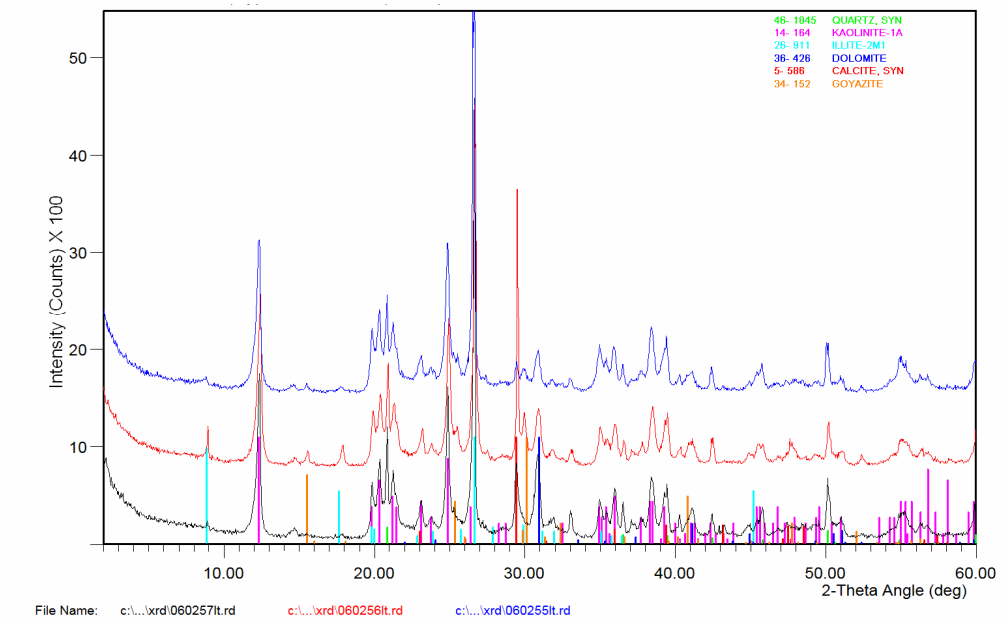


**Figure 4.2**: X-ray diffractograms of LTAs from samples from mines 2 (top), 4 and 6 (bottom).

**Table 4.6**: Mineralogy of <2 micron fraction by oriented aggregate XRD

| Mine Number | Kaolinite % | Illite % | Expandable Clay % | Nature of Expandable Clay |
|---|---|---|---|---|
| 1 | 93.00 | 1.00 | 6.00 | Mainly smectite |
| 2 | 92.00 | 3.00 | 5.00 | Mainly irregular I/S |
| 3 | 93.00 | 3.00 | 4.00 | Mainly irregular I/S |
| 4 | 96.00 | 0.00 | 4.00 | Mainly irregular I/S |
| 5 | 92.00 | 3.00 | 5.00 | Regular to irregular I/S |
| 6 | 90.00 | 2.00 | 8.00 | Smectite + regular I/S |

**Note**: I/S = interstratified (mixed-layer) illite-smectite

**Table 4.7**: Inferred ash chemistry ($SO_3$-free) based on Siroquant results

| Mine Number | 1 | 2 | 3 | 4 | 5 | 6 |
|---|---|---|---|---|---|---|
| $SiO_2$ | 55.17 | 59.32 | 56.18 | 51.33 | 57.57 | 54.02 |
| $Al_2O_3$ | 28.86 | 29.09 | 27.51 | 28.18 | 28.55 | 26.58 |
| $Fe_2O_3$ | 1.91 | 2.02 | 1.95 | 1.46 | 2.28 | 2.73 |
| $TiO_2$ | 3.22 | 1.74 | 1.92 | 1.23 | 1.19 | 0.99 |
| $P_2O_5$ | 0.41 | 0.67 | 1.10 | 1.26 | 0.57 | 0.38 |
| CaO | 6.27 | 3.93 | 7.27 | 12.20 | 5.98 | 10.27 |
| MgO | 2.69 | 1.63 | 3.08 | 2.70 | 2.66 | 4.13 |
| $Na_2O$ | 0 | 0 | 0 | 0 | 0 | 0 |
| $K_2O$ | 1.47 | 1.61 | 0.99 | 1.64 | 1.20 | 0.91 |

### 4.3.2 Coal Quality Predictor model results for six coals and their density fractions from the different Highveld coal mines

The van Alphen Consultancy Coal Quality Predictor model, which is also based on the chemical analysis (proximate, ultimate and elemental analyses) of the mineral matter and organic matter present in the coal, was used to estimate the proportions of minerals in the composite sample float and sink fractions. The composite feed coal samples were measured by CCSEM. The following general trends of results presented in Tables 4.8-4.10 are noted:

- Mineralogical analysis of coals which was predicted by the CQP model, shows that sample from mine 3 is distinct from the other samples analysed. The elevated proportion of ash yield in sample from mine 3 is attributed to the substantially

higher proportion of kaolinite and quartz present in the rock fragments (mudstone, sandstone and siltstone).

This coal contains significantly higher proportion of calcite along with the lowest proportion of pyrite. Significant proportions of pyrite and calcite in the coal occur as included particles in the carbon matrix and not as coarse cleat fragments. The coal contains a significantly high proportion of secondary aluminium sulphate compared to the other coals. The density results for this coal indicated that this coal probably has the highest proportion of rock fragments, indicating contamination by the stones from the roof and floor during mining.

- The model results also reveal that the sample from mine 1 contains significantly higher proportions of pyrite and siderite/Fe-oxide in comparison with the other coals. A significant proportion of the pyrite occurs as included fine grains in carbon-rich coal particles, in pyrite-rich layers, in carbon-rich particles and is also associated with quartz.
- Samples from mines 5 and 6 contain comparatively high proportions of pyrite and low proportions of kaolinite. In this coal, a significant proportion of the pyrite occurs as coarse pyrite cleat fragments, concentrated in the sink fraction. These two samples also have the highest proportion of coarse calcite particles that occur as cleat fragments. The sample from mine 5 has the highest proportions of quartz and microcline that are attributed to a higher proportion of coarse grained quartz/kaolinite/microcline sandstone rock fragments. The sample from mine 6 had the lowest ash yield with the correspondingly lowest proportion of "stone". The high proportion of extraneous coarse pyrite and calcite in samples from mines 5 and 6 can have an impact on obtaining representative samples if not treated with care during sample preparation. The sample from mine 2 has the highest kaolinite and illite/muscovite content. Excluding quartz, which occurs as the coarse sandstone rock fragments and included particles in the carbon-rich matrix, a high proportion of pyrite, calcite, dolomite and kaolinite occurs as included grains in the carbon-rich coal particles.
- The sample from mine 4 has the same mineralogical and chemical properties as the sample from mine 3.

Significantly higher proportions of illite, kaolinite, muscovite, siderite and quartz, along with a low proportion of carbon-rich particles, reported to the sink fractions (Table 4.10); whereas significantly higher proportions of dolomite, calcite, carbon-rich particles and low

proportions of illite, kaolinite and quartz, reported to the float fractions (4.9). Significant proportions of dolomite and calcite fluxing elements-bearing minerals in samples from mines 3 and 4 can react with kaolinite and illite in the carbon-rich particles at elevated temperatures to form a melt during coal gasification. This melt will result in the clinker formation.

**Table 4.8:** Proportions of minerals in coal composite from Highveld coal mines determined by CQP (mass %)

| **Mine** | **1** | **2** | **3** | **4** | **5** | **6** |
|---|---|---|---|---|---|---|
| Pyrite/pyrrhotite | 2.03 | 1.10 | 0.99 | 1.07 | 1.09 | 0.57 |
| Calcite | 2.48 | 2.34 | 3.09 | 2.78 | 1.68 | 2.43 |
| Dolomite | 2.90 | 3.31 | 3.68 | 3.99 | 2.79 | 2.96 |
| Apatite | 0.22 | 0.71 | 0.47 | 0.66 | 0.63 | 0.40 |
| Microcline | 0.12 | 0.24 | 0.24 | 0.30 | 0.18 | 0.09 |
| Muscovite | 0.50 | 0.99 | 0.99 | 1.34 | 0.82 | 0.37 |
| Illite | 0.74 | 1.47 | 1.47 | 1.98 | 1.21 | 0.55 |
| Kaolinite | 15.95 | 21.40 | 18.12 | 18.26 | 15.02 | 13.80 |
| Quartz | 5.11 | 2.87 | 3.72 | 1.56 | 1.27 | 3.24 |
| Siderite/Fe-oxide | 0.00 | 0.00 | 0.00 | 0.00 | 0.00 | 0.00 |
| Rutile | 0.37 | 0.33 | 0.30 | 0.42 | 0.24 | 0.35 |
| #Coal | 69.59 | 65.24 | 66.93 | 67.64 | 75.06 | 75.25 |

**Note:** #Coal – refers the carbon-rich matrix and represents the macerals

**Table 4.9:** Proportions of minerals in float fraction of coals from Highveld coal mines determined by CQP (mass %)

| Mine | 1 | 2 | 3 | 4 | 5 | 6 |
|---|---|---|---|---|---|---|
| Pyrite/pyrrhotite | 2.15 | 1.11 | 0.92 | 1.12 | 1.64 | 0.96 |
| Calcite | 2.92 | 2.58 | 3.59 | 3.73 | 2.71 | 3.66 |
| Dolomite | 1.53 | 1.48 | 2.18 | 1.86 | 1.24 | 1.67 |
| Apatite | 0.21 | 0.57 | 0.42 | 0.63 | 0.65 | 0.38 |
| Microcline | 0.18 | 0.25 | 0.27 | 0.30 | 0.26 | 0.11 |
| Muscovite | 0.80 | 1.02 | 1.13 | 1.33 | 1.17 | 0.45 |
| Illite | 1.18 | 1.50 | 1.67 | 1.97 | 1.73 | 0.67 |
| Kaolinite | 15.56 | 21.68 | 20.19 | 19.27 | 17.61 | 14.62 |
| Quartz | 6.07 | 5.17 | 6.18 | 3.83 | 5.91 | 5.36 |
| Siderite/Fe-oxide | 0.00 | 0.00 | 0.00 | 0.00 | 0.00 | 0.00 |
| Rutile | 0.27 | 0.34 | 0.39 | 0.40 | 0.28 | 0.28 |
| #Coal | 69.12 | 64.29 | 63.05 | 65.57 | 66.81 | 71.85 |

**Note:** #Coal – refers the carbon-rich matrix and represents the macerals

**Table 4.10:** Proportions of minerals in sink fraction of coals from Highveld coal mines determined by CQP (mass %)

| Mine | 1 | 2 | 3 | 4 | 5 | 6 |
|---|---|---|---|---|---|---|
| Pyrite/pyrrhotite | 5.31 | 2.66 | 2.47 | 6.48 | 6.08 | 9.21 |
| Calcite | 2.48 | 2.35 | 4.30 | 5.33 | 5.47 | 14.09 |
| Dolomite | 1.27 | 1.03 | 1.40 | 1.32 | 1.54 | 1.55 |
| Apatite | 0.06 | 0.24 | 0.26 | 0.69 | 0.39 | 0.44 |
| Microcline | 1.09 | 0.89 | 0.62 | 0.65 | 1.12 | 0.50 |
| Muscovite | 4.74 | 3.55 | 2.47 | 2.94 | 5.67 | 2.28 |
| Illite | 7.01 | 5.25 | 3.65 | 4.35 | 8.39 | 3.38 |
| Kaolinite | 37.98 | 44.94 | 40.38 | 40.18 | 25.24 | 27.74 |
| Quartz | 24.86 | 23.18 | 22.05 | 15.81 | 31.22 | 17.43 |
| Siderite/Fe-oxide | 2.16 | 1.36 | 1.14 | 1.30 | 2.49 | 1.75 |
| Rutile | 0.80 | 0.84 | 1.03 | 0.90 | 0.52 | 0.68 |
| #Coal | 12.23 | 13.71 | 20.24 | 20.05 | 11.87 | 20.95 |

**Note:** #Coal – refers the carbon-rich matrix and represents the macerals

### 4.3.3 Mineral matter in feed coal and their transformation at elevated Temperatures

The XRD analysis (Table 4.11) of the low temperature ash sample of the feed coal shows that this coal contains around 35% mineral matter (LTA), made up mainly of kaolinite (53%), quartz (18.2%) and dolomite (11.2%), with minor proportions of illite (5.6%), calcite (2.7%), pyrite (2.8%), and the phosphate minerals apatite ($Ca_5F(PO_4)_3$) (1.0%) and gorceixite ($BaAl_3(PO_4)_2(OH)_5.H_2O$) (1.9%). The presence of a small proportion of bassanite ($CaSO_4.½H_2O$) (2.2%) in the LTA sample produced from the feed coal probably formed from interaction of organically-associated calcium in the coals with organic sulphur during the low-temperature ashing process. Such a mineral assemblage confirmed the previous results for the South African coals that were found by Pinetown et al. (2006).

Data on the different size and density fractions, also summarised in Table 4.11, indicate that the float fractions, with low percentages of LTA, have a mineral assemblage with lesser proportions of quartz and pyrite than the LTA-rich sinks fractions. Dolomite, by contrast, is more abundant in the floats fractions than in the high-density sinks material. Together with the greater abundance of dolomite in the fine fractions than the coarse fractions, this suggests a relatively intimate association of the carbonate minerals with the maceral components. Apart from a greater abundance of illite in the coarse floats material, the clay minerals, the phosphates and the bassanite all appear to be more or less evenly distributed amongst the different size and density fractions.

**Table 4.11:** Mineralogy of LTA isolated from feed coal and float-sink fractions (wt %)

| Sample | Feed Coal | Coarse Floats | Coarse Sinks | Fine Floats | Fine Sinks |
|---|---|---|---|---|---|
| *LTA* | *34.6* | *15.0* | *55.4* | *14.9* | *53.6* |
| Quartz | 18.2 | 9.3 | 19.8 | 11.1 | 24.7 |
| Kaolinite | 53.3 | 61.0 | 58.8 | 62.8 | 49.0 |
| Illite | 5.6 | 13.8 | 5.9 | 4.8 | 7.3 |
| Calcite | 2.7 | | | | |
| Dolomite | 11.2 | 7.8 | 2.8 | 10.2 | 6.5 |
| Pyrite | 2.8 | 1.5 | 5.5 | 0.3 | 4.8 |
| Bassanite | 2.2 | 4.5 | 5.2 | 9.3 | 5.2 |
| Rutile | 1.1 | | 0.8 | 0.3 | 0.5 |
| Gorceixite | 1.9 | 2.1 | 1.4 | 1.3 | 1.9 |
| Apatite | 1.0 | | | | |

The high temperature-XRD results (Appendix G) for the LTA sample from Sasol coal feedstock to gasification, LTA of the sink fraction (>1.5635g/cm$^3$) and LTA of the float fraction (<1.5635g/cm$^3$) indicate that bassanite ($CaSO_4.1/2H_2O$), which was formed from the interaction of the organic sulphur and organic calcium or calcium-bearing minerals (calcite and dolomite) as well as from pyrite, decomposes at a low temperature of 400°C (Table G1). As expected kaolinite loses its water of hydration around 600°C (Table G1) to form amorphous meta-kaolin. Calcite and dolomite that are not pure minerals in the coal, decompose at 600°C (Table G1) and some of their oxides will react with aluminium silicate to form a melt. Interestingly, for all ash samples tested, quartz grains persist to 1300°C and lose their natural structure at 1350°C during HT-XRD analysis. The HT-XRD analysis also reveals that anorthite, which crystallises from the melt, appears at 1100°C and persists to 1400°C (Table G1). For the LTA from Sasol coal feedstock as well as LTA from the float fraction, cristobalite which is formed from clays at elevated temperatures appears at 1200-1400°C (Table G1). The HT-XRD analysis of LTA from the sink fraction indicated that mullite, which is formed from high temperature transformation of either kaolinite or K-feldspar, appears at 900°C and persists to 1250°C.

### 4.3.4 CCSEM and SEM-EDS analyses of coals

The CCSEM analysis (Table 4.12) confirms that the coal sample analysed in this study contains the major minerals: kaolinite ($Al_2Si_2O_5(OH)_4$), quartz ($SiO_2$), muscovite/illite ($K_2O.3Al_2O_3.6SiO_2.2H_2O/K_{1.5}Al_4(Si_{6.5}Al_{1.5})O_{20}(OH)_4$), calcite ($CaCO_3$), dolomite ($CaMg(CO_3)_2$) and pyrite ($FeS_2$). Minor and trace minerals are orthoclase, apatite, rutile, and Fe-oxide/siderite ($Fe_2O_3/FeCO_3$), zircon ($ZrSiO_4$), monazite (Ce, La, Th) $PO_4$ and Nd-Ce-Al-Th-phosphate.

The selected back-scattered electron images taken during CCSEM analysis of the feed coal taken from the coal conveyor belts entering the gasifier (Figure 4.3) highlight mineral attributes. From Figures 4.3 and 4.5 it is clear that the following particle types and associated minerals are present in the coal sample:

Organic-rich coal particles with small concentrations of kaolinite (particle A), quartz (particle A), pyrite (particle A1) and calcite/dolomite inclusions. Fine to coarse dolomite and calcite cleats in predominantly organic-rich particles (particle A2) are common.

- Coarse to fine quartz-rich sandstone rock fragments (particles B, E and E1). Minor kaolinite, microcline, muscovite and fine pyrite inclusions are present.

- Large (>750µm) calcite and pyrite cleat fragments (particle D).
- Fine grained kaolinite-rich mudstone/siltstone rock fragments. Minor muscovite, quartz and orthoclase (particle F) are present.

The black carbon-rich particles shown in Figure 4.3 are vitrinite and the grey carbon-rich phases are inertinite-rich (Ag).

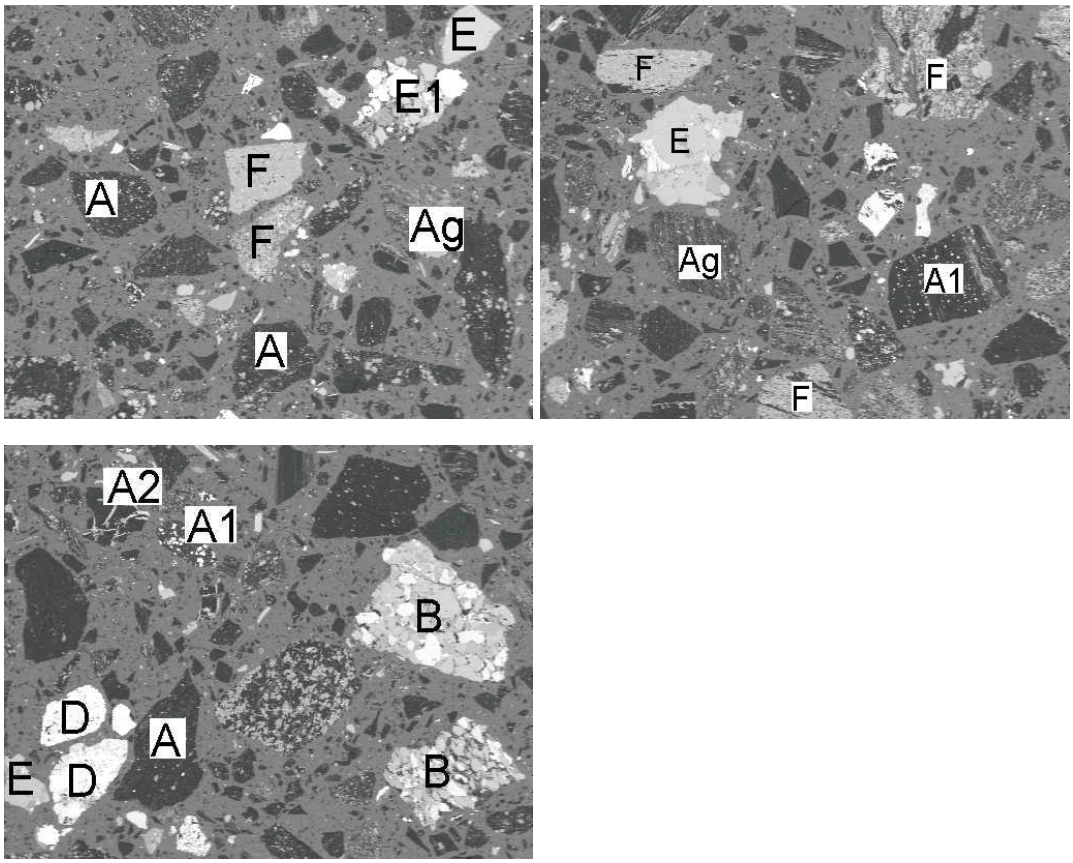


**Figure 4.3**: Scanning electron micrographs (back-scattered electron images) highlighting mineral attributes and deportment characteristics in Gasifier feedstock. Carbon-rich particles are black, mineral matter is light grey to white and epoxy mounting resin is grey. The width of each image is approximately 3.5mm.

The XRD and CCSEM results (mass percentages of minerals) are presented in Table 4.12. Kaolinite and to a lesser extent quartz, are the major coal minerals (Table 4.12). Pyrite, calcite, dolomite, muscovite/illite and feldspar are minor minerals. The calculated elemental proportions derived from the CCSEM mineral proportions agreed well with the XRF ash elemental proportions, whereas the XRD analysis indicated higher Si, Ti and K and lower Al, Mg and Fe than the XRF results (as reported in Paragraph 4.1.3). The quantitative XRD results given in Table 4.12 are based on the total amounts of the crystalline phases present in the coal sample. The CCSEM results (Table 4.12) are in broad agreement with the QEMSCAN measurements (Paragraph 4.3.5).

**Table 4.12**: Mineral abundance in coal (mass %)

| Mineral | Idealised formula | CCSEM Mass% | XRD analysis |
|---|---|---|---|
| Pyrite | $FeS_2$ | 2.10 | 3.80 |
| Quartz | $SiO_2$ | 5.30 | 28.00 |
| Feldspar | $KAlSi_3O_8$ | 1.80 | nd |
| Muscovite/illite | $K_2O.3Al_2O_3.6SiO_2.2H_2O$/ $K_{1.5}Al_4(Si_{6.5}Al_{1.5})O_{20}(OH)_4$ | 2.90 | 13.00 |
| Kaolinite | $Al_2Si_2O_5(OH)_4$ | 17.10 | 34.00 |
| Iron oxide/siderite | $Fe_2O_3/FeCO_3$ | 0.02 | 0.60 |
| Calcite | $CaCO_3$ | 2.10 | 7.80 |
| Dolomite | $CaMg(CO_3)_2$ | 2.30 | 9.00 |
| Ankerite | $(Fe, Ca, Mg)CO_3$ | 0.09 | nd |
| Apatite | $Ca_5F(PO_4)_3$ | 0.20 | nd |
| Anatase/rutile | $TiO_2$ | 0.40 | 3.1 |
| Other | Unidentified minerals | 0.09 | nd |
| Coal | Organic fraction | 65.57 | nd |
| Total | | 100.0 | 99.30 |

**Note:** nd: not detected

The SEM-EDS analysis (Figure 4.4) of the coal sample taken from the gasifier during the dig-out test confirmed that carbonate cleats (dolomite and calcite) occurred within carbon-rich particles in this coal sample. The typical X-ray spectra of kaolinite and potassium-feldspar contained in the dig-out samples are given in Figures E1and E2 respectively. In most cases, the fluxing elements-bearing minerals such as dolomite and calcite are associated with each other in the coal samples analysed in the present study. These results are in good agreement with QEMSCAN results (Figure 4.7). These included minerals that contain the fluxing elements (Ca and Mg) (Appendix E, Figures E3 and E4) are also associated with the included kaolinite. The SEM-EDS analysis (Figure 4.4 and Figure E5) also shows that pyrite grains (white) are included in the carbon particles and some are associated with kaolinite in the coal sample.

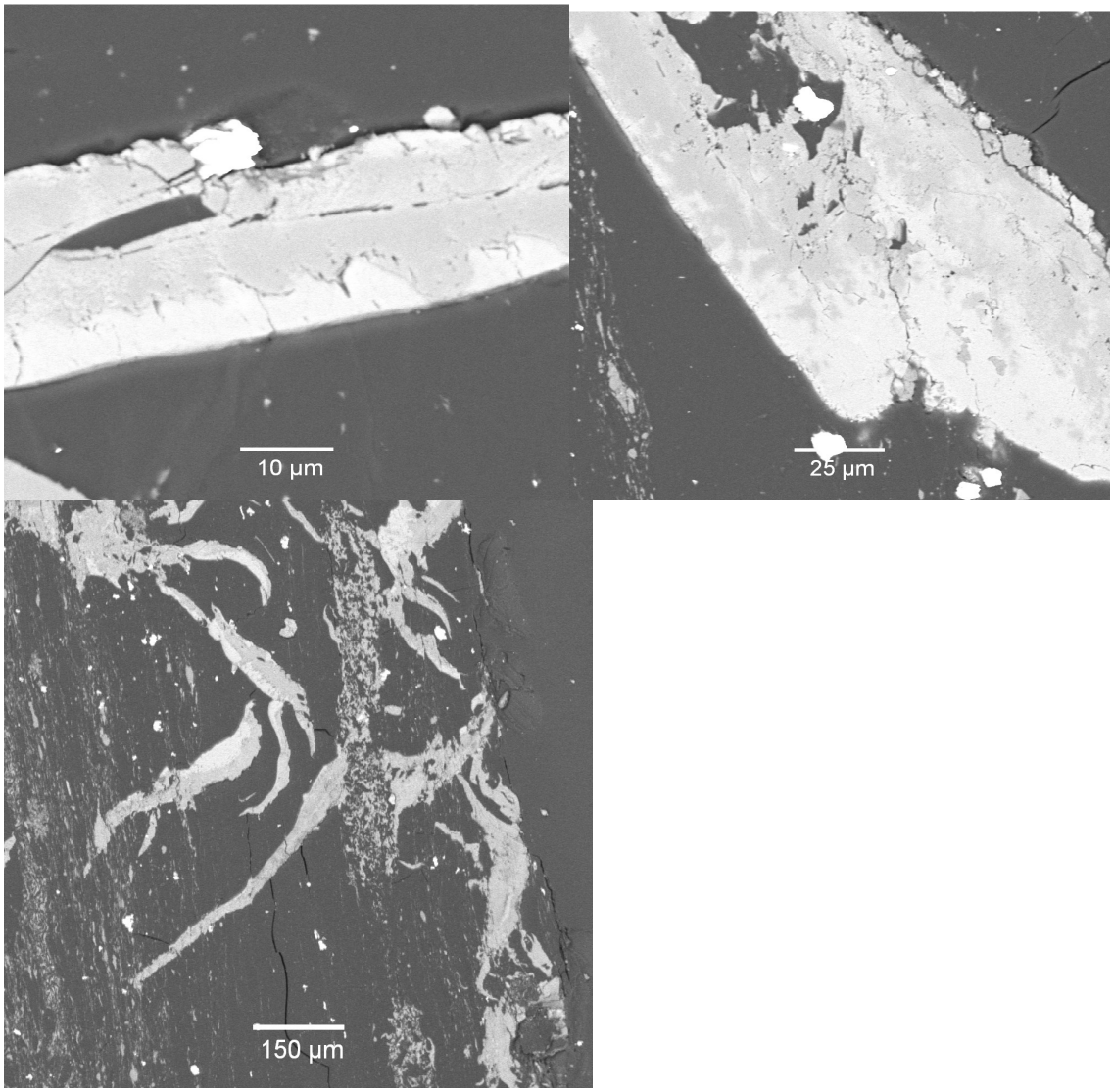


**Figure 4.4:** The BSE images of feed coal show carbonate cleats (calcite with white colour and dolomite with light grey) between two carbon particles, the bottom image shows included kaolinite associated with dolomite/calcite, kaolinite is also associated with dolomite/calcite/pyrite (white dots). Scale bar of the top left image is 10µm, for the top right image it is 25µm, and for the bottom image it is 150µm.

Figure 4.5 shows that grains of quartz with grey appearance, kaolinite (dark grey), potassium feldspar (light grey) and white pyrite grains are contained in the extraneous rock fragments analysed in this study. Kaolinite in the rock fragments is expected to transform differently in comparison with the kaolinite mineral associated with dolomite/calcite/ pyrite in the coal during coal combustion/gasification.

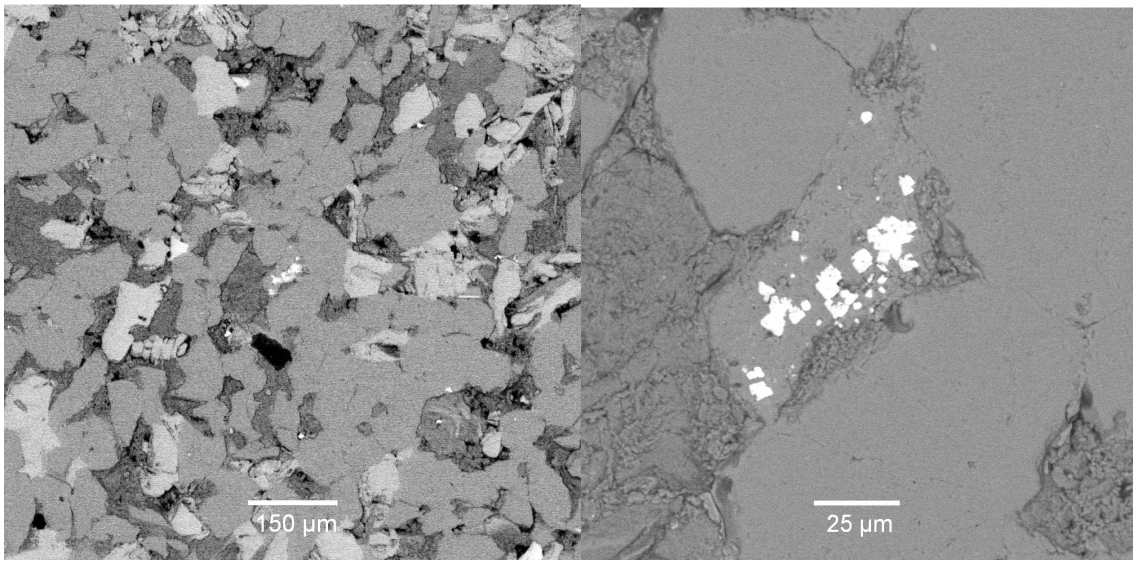


**Figure 4.5:** Back-scattered electron images of dig-out coal stone (from feed coal): Quartz grains (mid-grey), kaolinite (dark grey), potassium feldspar (light grey) and pyrite grains (white). Scale bar of the first image is 150µm, while for the second image it is 25µm.

### 4.3.5 QEMSCAN analysis of feed coal

QEMSCAN analysis of sample 32T (feed coal) indicates that high proportions of kaolinite (15.81%), quartz (6.5%), dolomite (2.67%), calcite (2.18%), organic matter (68.76%) and low proportions of pyrite (1.63%), siderite (0.02%), rutile (0.94%), illite (0.42%), apatite (0.07%) and organic sulphur (0.94%) are contained in these samples. The size of the mineral grains in the coal sample 32T analysed in this study ranged from 10 -106 microns

False-colour images of grains of minerals in Figure 4.6 indicate the occurrence of minerals in the coal particles. As shown in this figure, some pyrite particles (yellow) occur as extraneous particles while others are associated with minerals such as kaolinite, quartz and also carbon-rich (black) particles.

From Figure 4.7 the amount of transitions was normalised to a 100%. The iDiscover (QEMSCAN programme) counted the transitions between the minerals that are present in the sample. The transitions were converted to a percentage, meaning that out of the total number of transitions in the sample, a percentage between a specific combination of minerals (in this case between background and a set of minerals) was displayed. This figure shows mineral associations in the coal sample 32T.

The background mentioned in Figure 4.7 is the mounting medium. Depending on the sample type, the mounting medium can vary between wax and epoxy resin. With regards

to the background transitions, the transitions between background and mineral can be seen as a proxy for liberation.

QEMSCAN analysis of the coal sample in this figure shows the following:
Some pyrite particles are strongly associated with both high sulphur coal (organically-bound sulphur) and carbon-rich fraction (maceral). They are also associated with the background, indicating that around 30% of the surface of pyrite grains are excluded.

- All feldspar particles in this coal sample are included (associated with the carbon-rich fraction and not with the background) and are strongly associated with calcite and dolomite. A small proportion of illite is associated with the background, indicating that around <5% of the surface of illite grains is excluded. A small proportion of illite is associated with quartz and organic sulphur, while a significant proportion is associated with kaolinite.
- The apatite grains are strongly associated with calcite and carbon-rich fraction and are not associated with the background, indicating that the apatite grains are included.
- Interestingly, about 30% dolomite particles are associated with calcite grains and a significant proportion (above 50%) with the carbon-rich fraction. The results also show that a small proportion of dolomite grains are associated with the background, indicating that around 3% of dolomite particles are excluded. This mineral association could affect the melting of mineral matter in the coal at elevated temperatures and pressure during coal gasification or combustion.
- Calcite grains (above 50%) are strongly associated with the carbon-rich fraction (see also Figure 4.4) and are also associated with dolomite, kaolinite, quartz and apatite. Due to the presence of the fluxing elements-bearing minerals in the coal, this mineral association could contribute significantly to the sintering and slagging of mineral matter at elevated temperatures during coal gasification or combustion. The calcite particles are also associated with the background, indicating that about 5% of the surface of calcite grains is excluded.
- In most cases, the organic sulphur is associated with carbon-rich particles (macerals) in the coal. The electron microprobe results in Table 4.13 corroborate this result. The organic sulphur particles interacted with the organically-associated calcium in the coals to form bassanite ($CaSO_4.½H_2O$) during the low-temperature ashing process (Table 4.5).

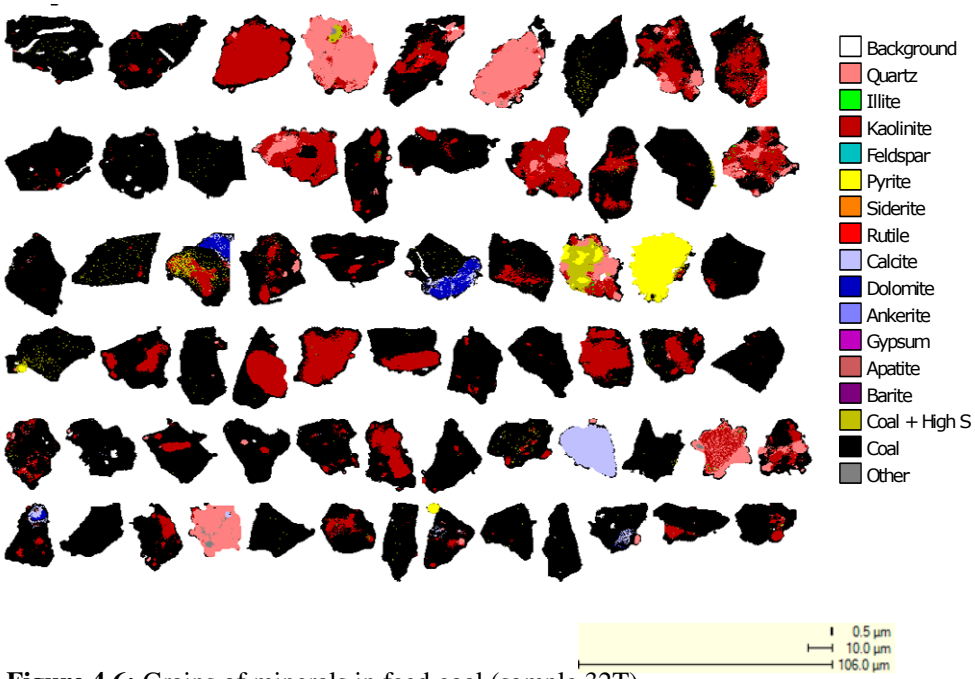


**Figure 4.6:** Grains of minerals in feed coal (sample 32T).

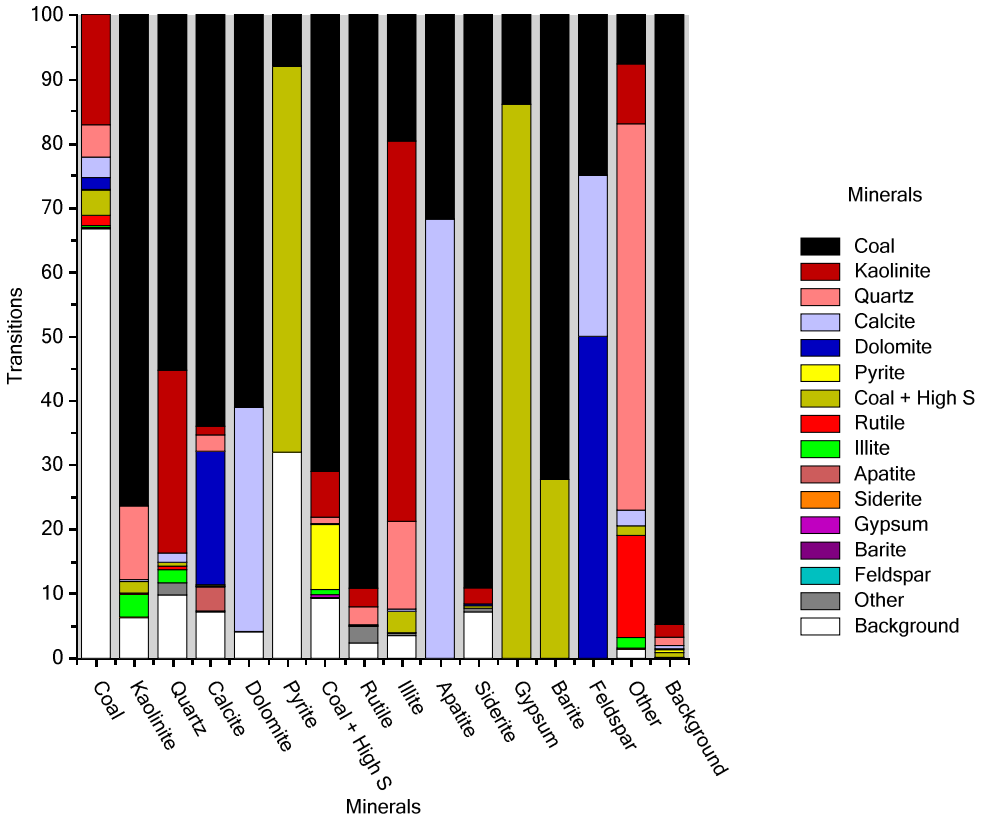


**Figure 4.7:** Mineral associations of feed coal (sample 32T).

## 4.4 Elemental composition of individual coal macerals by electron microprobe

As was stated earlier in Chapter 3 of this thesis, the organically-bound inorganic elements, as well as sub-micron minerals in the macerals, could interact with each other or react with aluminium silicates at elevated temperatures under reducing and oxidising conditions to form a melt. The qualification and quantification of this mineral matter in the organic matter (macerals) in the coal samples (using electron microprobe and optical microscope), were used to test the hypothesis (that the interactions between the organically-bound inorganic elements and sub-micron clays at elevated temperatures, give rise to the sintering and slagging of mineral matter during either coal combustion or gasification) which is stated in Chapter 3.

Table 4.13 contains a summary of the results of the electron microprobe analyses of the coal macerals. These results represent the average proportion of each element in each maceral of the respective sample analysed in this study, based on the number of individual points indicated in each case.

Ward (1998, 2005) found that the vitrinite macerals in the Australian coals contained lower carbon and higher oxygen contents than the inertinite macerals. The same author also found that telocollinite (also referred to in some standards as collotelinite) generally has a slightly lower carbon content than the desmocollinite in the same coal sample. Comparison with results presented by Ward et al. (2005) indicates that the carbon content of the telocollinite in most samples (around 75%) is similar to that of the telocollinite in coals from the Bowen Basin of Australia, having a mean maximum vitrinite reflectance of around 0.7%. Similar vitrinite reflectance values are noted in the South African coal samples analysed in the present study.

The telocollinite in sample from mine 6, however, has a slightly lower carbon content (around 70%), yet still has a vitrinite reflectance of 0.7%. The significance of this is not clear at the present time; it may indicate either a slightly low vitrinite carbon percentage for a coal with a similar rank level to the other samples, or it may indicate a slightly high reflectance for the vitrinite in a coal with a slightly lower rank level.

The electron probe analysis of coals revealed that the vitrinite macerals in each individual coal contains significantly higher proportions of the organic sulphur and nitrogen, in comparison with the inertinite macerals in the same coal samples. These results are in agreement with the previous results obtained by Ward et al. (2005) and Gurba (2001). In almost all cases, the proportion of these elements in the vitrinite macerals is approximately twice that in the same sample's inertinite components.

The proportion of organic sulphur in the vitrinite of samples from mines 1, 2, 3 and 5 is around 0.6-0.8%, while samples from mines 4 and 6 have only 0.4-0.5% organic sulphur. The significance of this observation is also not clear at the present time. From the results given in Table 4.13, it is clear that coal macerals contain no organically-bound iron. The absence of any significant iron in these macerals confirms that the sulphur in all cases is organic in nature, and that the higher sulphur levels do not reflect incorporation of sub-microscopic pyrite in the macerals concerned. The difference between these values and the total sulphur content of the coals (Table 4.2), reflects the additional occurrence of pyrite (pyritic sulphur), as indicated by the mineralogical data in Table 4.5.

Despite efforts to avoid including data form points with significant contamination by mineral matter, the vitrinite and semi-fusinite macerals in sample from mine 3, and possibly also sample from mine 4, appear to contain small (approximately equal) proportions of both Al and Si. This may suggest incorporation of an intimate admixture of sub-micron kaolinite or a similar clay mineral into the maceral structure. Lesser, but similarly equal, proportions of Al and Si are noted in the vitrinite of samples from mines 1 and 2. The vitrinite in samples from mines 5 and 6 appears to contain relatively high proportions of Al and only traces of Si, suggesting either incorporation of bauxite-group minerals (gibbsite and/or boehmite), or possibly incorporation of Al as an inorganic element within the vitrinite structure.

Inertinite macerals in some coals analysed contain small proportions (mostly <0.2%) of Ca. Ca is especially abundant in the sporinite and inertinite components of sample from mine 6, probably indicating traces of calcite or dolomite in the pore spaces of those particular macerals. For the vitrinite macerals, the relatively minor amount of Ca may occur within the organic structure.

It is interesting to note that the vitrinite in samples from mines 1, 2, 3 and 4 contains significant proportions (0.3-0.5%) of titanium in comparison with other coal samples analysed in this study. The significant proportion of titanium in these coal samples detected by the electron microprobe, may occur either as the organically-associated inorganic element or evenly distributed sub-microscopic particles in the coal vitrinite. The vitrinites in the other two coal samples possibly contain small proportion of Ti (<0.1%). Interestingly, the electron microprobe results for the selected area of inertinite macerals, show that titanium is however, not present in any of these inertinite components.

According to Li et al. (2006) more detailed electron microprobe analysis, using element mapping techniques, has shown that Ca and Al in other coals form an integral part of the maceral structure, rather than representing fine (but discrete) included mineral particles. These techniques have however, not been applied to the coals of the present study, nor to Ti in other coal samples.

**Table 4.13:** Elemental composition of macerals in coal samples from the different mines by electron microprobe analysis

| Maceral | Pts | C% | N% | O% | Mg% | Al% | Si% | S% | K% | Ca% | Ti% | Fe% |
|---|---|---|---|---|---|---|---|---|---|---|---|---|
| **Mine 1** | | | | | | | | | | | | |
| TC | 23 | 73.24 | 2.38 | 18.97 | 0.01 | 0.06 | 0.06 | 0.65 | 0.00 | 0.10 | 0.55 | 0.02 |
| DSC | 12 | 74.82 | 2.46 | 17.39 | 0.01 | 0.10 | 0.11 | 0.67 | 0.01 | 0.10 | 0.44 | 0.00 |
| SF | 15 | 84.40 | 0.98 | 10.21 | 0.01 | 0.02 | 0.04 | 0.30 | 0.01 | 0.07 | 0.02 | 0.00 |
| FUS | 16 | 85.73 | 0.84 | 8.68 | 0.03 | 0.06 | 0.09 | 0.25 | 0.01 | 0.13 | 0.01 | 0.00 |
| **Mine 2** | | | | | | | | | | | | |
| TC | 23 | 74.34 | 2.29 | 18.00 | 0.03 | 0.10 | 0.07 | 0.79 | 0.01 | 0.13 | 0.38 | 0.00 |
| DSC | 22 | 78.56 | 1.94 | 14.71 | 0.01 | 0.09 | 0.12 | 0.58 | 0.01 | 0.06 | 0.22 | 0.00 |
| SF | 7 | 88.28 | 0.23 | 7.07 | 0.07 | 0.01 | 0.01 | 0.24 | 0.01 | 0.07 | 0.01 | 0.00 |
| FUS | 15 | 89.28 | 0.75 | 6.31 | 0.07 | 0.02 | 0.02 | 0.36 | 0.01 | 0.15 | 0.01 | 0.00 |
| **Mine 3** | | | | | | | | | | | | |
| TC | 15 | 73.17 | 2.41 | 19.83 | 0.01 | 0.41 | 0.33 | 0.76 | 0.05 | 0.06 | 0.38 | 0.00 |
| DSC | 12 | 74.49 | 2.31 | 18.62 | 0.01 | 0.40 | 0.25 | 0.77 | 0.08 | 0.07 | 0.41 | 0.00 |
| SF | 10 | 81.04 | 1.66 | 13.03 | 0.02 | 0.22 | 0.25 | 0.42 | 0.02 | 0.08 | 0.01 | 0.00 |
| FUS | 14 | 83.11 | 1.00 | 11.41 | 0.02 | 0.00 | 0.01 | 0.36 | 0.00 | 0.11 | 0.02 | 0.00 |
| **Mine 4** | | | | | | | | | | | | |
| TC | 23 | 77.32 | 1.93 | 16.02 | 0.01 | 0.10 | 0.10 | 0.39 | 0.03 | 0.06 | 0.42 | 0.00 |
| DSC | 17 | 77.67 | 2.10 | 15.24 | 0.01 | 0.17 | 0.16 | 0.40 | 0.02 | 0.07 | 0.45 | 0.00 |
| SF | 12 | 85.46 | 0.81 | 9.16 | 0.02 | 0.01 | 0.01 | 0.19 | 0.01 | 0.09 | 0.01 | 0.00 |
| FUS | 14 | 86.36 | 0.99 | 8.43 | 0.04 | 0.01 | 0.02 | 0.18 | 0.01 | 0.17 | 0.01 | 0.00 |
| **Mine 5** | | | | | | | | | | | | |
| TC | 33 | 75.39 | 2.10 | 17.96 | 0.01 | 0.24 | 0.07 | 0.80 | 0.01 | 0.09 | 0.03 | 0.00 |
| DSC | 19 | 76.47 | 2.19 | 16.80 | 0.01 | 0.17 | 0.09 | 0.87 | 0.01 | 0.08 | 0.09 | 0.00 |
| SP | 1 | 79.70 | 1.89 | 15.00 | 0.02 | 0.54 | 0.53 | 1.14 | 0.02 | 0.04 | 0.03 | 0.00 |
| SF | 6 | 86.26 | 0.94 | 9.48 | 0.06 | 0.06 | 0.08 | 0.34 | 0.01 | 0.17 | 0.01 | 0.00 |
| FUS | 8 | 89.22 | 0.43 | 7.39 | 0.04 | 0.09 | 0.07 | 0.37 | 0.01 | 0.12 | 0.00 | 0.00 |
| IDT | 2 | 90.90 | 1.52 | 5.77 | 0.02 | 0.13 | 0.13 | 0.33 | 0.00 | 0.12 | 0.02 | 0.00 |
| **Mine 6** | | | | | | | | | | | | |
| TC | 29 | 69.51 | 2.67 | 23.38 | 0.02 | 0.19 | 0.06 | 0.46 | 0.01 | 0.12 | 0.07 | 0.00 |
| DSC | 21 | 70.06 | 2.55 | 22.06 | 0.02 | 0.20 | 0.08 | 0.47 | 0.01 | 0.17 | 0.06 | 0.00 |
| CUT | 2 | 76.49 | 1.61 | 16.03 | 0.01 | 0.18 | 0.01 | 0.35 | 0.00 | 0.12 | 0.02 | 0.00 |
| SP | 4 | 77.04 | 1.84 | 14.28 | 0.02 | 0.29 | 0.09 | 0.36 | 0.00 | 0.93 | 0.02 | 0.00 |
| SF | 18 | 80.39 | 1.25 | 12.64 | 0.02 | 0.04 | 0.03 | 0.22 | 0.01 | 0.14 | 0.01 | 0.01 |
| FUS | 12 | 85.05 | 0.72 | 9.40 | 0.06 | 0.10 | 0.10 | 0.17 | 0.00 | 0.26 | 0.01 | 0.00 |
| IDT | 5 | 90.13 | 0.68 | 4.23 | 0.02 | 0.02 | 0.01 | 0.20 | 0.00 | 0.43 | 0.01 | 0.00 |

**Key:** TC = telocollinite, DSC = desmocollinite, SP = sporinite, CUT = cutinite, SF = semifusinite, FUS = fusinite, IDT = inertodetrinite. Pts = number of points analysed for indicated maceral.

## 4.5 Chemical fractionation method

Two South African low-grade, medium rank C bituminous (SAMB) feed coals (Highveld feed coal 1 and Highveld feed coal 2) to the conversion coal processes, were used in this study. Samples 1 and 2 were obtained from the same source and have similar chemical and physical properties. However, Highveld feed coal 1 was obtained from the top of the gasifier after its operation had ceased and had been exposed to temperatures of <400°C, while Highveld feed coal 2 was obtained from the conveyor belt entering the gasification plant, before heat treatment.

The preliminary results obtained from chemical, mineralogical and physical analyses of the two feed coals and residual coal particles from the pyrolysis experiments, using the conventional analytical techniques and results from ICP-OES analysis of each leachate obtained from the sequential leaching procedure, are discussed in this section.

### 4.5.1 Proximate analysis of feed coal before and after sequential leaching

Proximate analysis data (Table 4.14) indicate that the two Highveld feed coals before leaching (unleached coal 1(UC1) and unleached coal 2 (UC2)) had 19-22% volatile matter, 3.1-3.4% air-dried moisture content and an ash yield between 25% and 31%. Total sulphur content ranged from 1.0-1.5%. These results are in agreement with those previously found by (Pinheiro et al., 1998-1999; Matjie et al., 2006; DME, 2006). No significant changes were observed in the moisture and volatile matter contents after sequential leaching.

As might be anticipated, the ash yield of these samples decreased after ammonium acetate and acid leaching steps, due to removal of the relevant soluble inorganic components. No significant changes were observed in the volatile matter yield after sequential leaching. The fixed carbon content increased slightly after ammonium acetate and acid leaching, likely as a result of the reduction in ash percentage. The sulphur content was reduced after water leaching and then remained fairly constant through the ammonium acetate and acid leaching stages. This may in part reflect removal of iron sulphates derived from oxidation of pyrite in the coal samples, or alternatively removal of sulphate ions in the pore water derived from other sources.

**Table 4.14**: Proximate analyses (air-dried basis, %) of Highveld coal samples before and after sequential leaching with water, ammonium acetate and hydrochloric acid

| | Samples | Moisture (%) | Ash (%) | Volatile Matter (%) | Fixed Carbon (%) | Total Sulphur (%) |
|---|---|---|---|---|---|---|
| Coal 1 | HUC | 3.10 | 30.70 | 19.60 | 46.60 | 1.41 |
| | $H_2O$ | 3.20 | 29.50 | 20.30 | 47.00 | 1.17 |
| | $NH_4OAc$ | 3.10 | 27.50 | 19.30 | 50.10 | 1.15 |
| | HCl | 3.10 | 26.00 | 19.50 | 51.40 | 1.02 |
| Coal 2 | HUC | 3.40 | 25.10 | 21.90 | 49.60 | 1.03 |
| | $H_2O$ | 3.30 | 24.80 | 22.90 | 49.00 | 0.94 |
| | $NH_4OAc$ | 3.60 | 22.70 | 21.70 | 52.00 | 0.96 |
| | HCl | 4.00 | 20.60 | 21.80 | 53.60 | 0.96 |

**Note:** HUC = Highveld coals before sequential leaching test
$H_2O$ = after water leaching;
$NH_4OAc$ = after ammonium acetate leaching and
HCl = after hydrochloric acid leaching

### 4.5.2 Ultimate analysis of feed coal before and after leaching

The normalised ultimate analysis (Table 4.15) indicated that these coals had 77-80% carbon dry and 3.70-4.10% hydrogen with relatively low concentrations of sulphur (1.44-2.13%) and around 2% nitrogen. The oxygen content of the coals ranged from 13-14%. These results are in agreement with those previously found by (Pinheiro et al., 1998-1999; Matjie et al., 2006; DME, 2006). A minor increase in the carbon and hydrogen was noted after ammonium acetate leaching. Due to the presence of ammonium acetate in the residual coal particles, nitrogen contents were slightly higher after this leaching stage. The slight variation in the concentration of oxygen during the sequential leaching could perhaps be attributed to the dissolution of salts of carboxylic acids from the coals.

**Table 4.15:** Normalised ultimate analyses (dry ash-free basis, %) of Highveld coal samples before and after sequential leaching with water, ammonium acetate and hydrochloric acid

| | Samples | Carbon | Hydrogen | Nitrogen | Sulphur | Oxygen |
|---|---|---|---|---|---|---|
| Coal 1 | HUC | 78.99 | 3.93 | 2.02 | 2.13 | 12.93 |
| | $H_2O$ | 79.63 | 3.76 | 2.07 | 1.74 | 12.81 |
| | $NH_4OAc$ | 78.72 | 3.80 | 2.49 | 1.66 | 13.33 |
| | HCl | 77.98 | 3.67 | 2.21 | 1.44 | 14.70 |
| Coal 2 | HUC | 78.80 | 4.10 | 1.99 | 1.44 | 13.68 |
| | $H_2O$ | 78.94 | 3.89 | 1.97 | 1.31 | 13.88 |
| | $NH_4OAc$ | 79.40 | 3.95 | 2.54 | 1.30 | 12.81 |
| | HCl | 77.14 | 3.89 | 2.24 | 1.27 | 15.46 |

### 4.5.3 The normalised XRF and ICP-OES analyses for HTA samples produced from the coal samples 1 and 2 before and after the sequential leaching

The ICP-OES analyses of the High Temperature Ash (HTA) of coal samples 1 and 2 are shown in Appendix A, Table A2 and Table A3. In all cases, the normalised proportions of inorganic elements (XRF analysis) in the HTA, produced after heating the two coals (HUC1 and HUC2) at 815°C were very similar, thus confirming the applicability of the ICP data for samples (Table 4.16). Sulphur results are not reported, as the XRF method used was regarded as only semi-quantitative for sulphur. The ashes analysed by ICP-OES provided results on the Ba and Sr concentrations; these elements were not included in the typical XRF major elemental analysis routine.

It is clear from the results given in Tables 4.16 and 4.17, that HTA from coal 1 contained significantly higher proportions of iron and silicon oxides than HTA of coal 2. The variation in chemical composition of these two coals can be attributed to variations in the quality of coal with the depth of the seams. In most cases, results given in Tables 4.16 and 4.17 indicated that the percentages of some major elemental oxides for samples 1 and 2 are very similar from both ICP-OES and XRF analyses. However, the most abundant elements in the feed coals (as expressed as $SiO_2$ and $Al_2O_3$), are approximately 2% higher in the results from XRF than by ICP-OES analysis. Although there is a slight discrepancy of concentrations of both $SiO_2$ and $Al_2O_3$, these differences do not significantly affect the trends in the data series. The primary constituents in the SAMB feed coals are $SiO_2$,

$Al_2O_3$, CaO, $Fe_2O_3$, MgO and $TiO_2$. Minor proportions (<0.6%) of $K_2O$, $Na_2O$, $P_2O_5$, SrO, BaO and $Mn_3O_4$ were also present, along with a $SO_3$ content between 4.5 and 5.7%.

A decrease in the content of the inorganic elements present in the original coals during sequential leaching with water, ammonium acetate and hydrochloric acid solutions may be attributed to the decomposition of other coal minerals, dissolution of ions from moisture, as well as the loss of volatiles upon heat treatment. Carbonate minerals (dolomite and calcite), along with other organically-bound calcium and sulphur may dissolve in solutions of lixiviants (ammonium acetate and hydrochloric acid) during the leaching steps and therefore a significant decrease in the calcium, magnesium and sulphur data would result. Matjie et al. (2008) also found that the proportions of MgO, SrO and BaO correlated quite well with the proportion of CaO, suggesting on the basis of other studies (Ward et al., 1999) that they may be associated with the carbonate minerals in the Highveld coal samples.

Significant reductions in the concentrations of BaO, MgO, SrO and CaO upon leaching, as shown in Table 4.17, confirmed that Ba, Mg, Sr and Ca dissolved in the lixiviants used during the sequential leaching experiments. In addition, Miller and Given (1978); Benson and Holm (1985) and Benson (1987) showed that significant proportions of the Ca, Mg and Na in the lignite coal samples dissolved in ammonium acetate solution during the leaching experiments. These elements occurred mostly in ion-exchangeable form (possibly associated with carboxylate compounds and partly in the pore waters and an acid-soluble form) (Miller and Given, 1978; Benson and Holm, (1985); Benson, 1987). The electron probe analysis of Highveld coals reported in this section, confirmed the presence of calcium, iron and magnesium that are either in the form of salts of carboxylic acids (organically-bound inorganic elements) or associated with carbon-rich particles in the coal macerals.

Trace amounts of fluxing elements such as K, Sr and Fe that may also reduce ash fusion temperature (AFT) of mineral matter in the coal, were leached out from some coal samples evaluated in this study (Table 4.16). As expected, lower AFT's are due to the presence of fluxing elements-bearing minerals that have reacted with organically-associated inorganic elements and clays and may also be attributed to increased basic oxide levels and low $SiO_2/Al_2O_3$ ratios. The chemical fractionation results (Tables 4.16-4.18) also reveal that concentrations of $Na_2O$, $SO_3$ and $P_2O_5$ in HTA samples of the coals

decreased substantially during the sequential leaching steps of these coals. The dissolution of sodium in distilled water implies that most of the sodium ions were dissolved in the pore water within the coal. These results are in line with previous results that were found by Ward (1991).

A significant decrease of sulphur in the leached coal particles may be attributed to the formation of acidic ammonium sulphate through the reaction of organic sulphur or pyrite with ammonium acetate, as well as sulphuric acid formation because of the reaction of the partially oxidised pyrite and water. Ward (1991) suggested in his studies that sulphuric acid formed during oxidation of pyrite reacted with calcium from carbonate minerals and iron from the oxidised pyrite during the selective leaching steps. A slight reduction in the concentration of phosphorus from coals can be attributed to the reaction between phosphate minerals in the coal and ammonium sulphate produced from the ammonium acetate solution, as well as from HCl during the sequential leaching experiments.

**Table 4.16:** Inorganic oxide percentages from normalised XRF and ICP-OES analyses of HTA samples of Highveld coal sample 1 before and after leaching (wt %)

| | **ICP-OES Data** | | | | **XRF Data** | | | |
|---|---|---|---|---|---|---|---|---|
| | **HUC1** | **WL HLC1** | **AAL HLC1** | **HClL HLC1** | **HUC1** | **WL HLC1** | **AAL HLC1** | **HClL HLC1** |
| | **%** | **%** | **%** | **%** | **%** | **%** | **%** | **%** |
| $SiO_2$ | 54.68 | 54.69 | 62.01 | 61.09 | 56.74 | 56.68 | 61.65 | 61.09 |
| $Al_2O_3$ | 24.60 | 24.89 | 28.3 | 30.83 | 26.37 | 26.66 | 29.12 | 31.6 |
| $Fe_2O_3$ | 5.61 | 5.22 | 5.54 | 3.84 | 5.89 | 5.37 | 5.61 | 3.66 |
| $TiO_2$ | 1.46 | 1.48 | 1.67 | 1.84 | 1.51 | 1.54 | 1.64 | 1.83 |
| BaO | 0.15 | 0.16 | 0.17 | 0.3 | * | * | * | * |
| SrO | 0.20 | 0.21 | 0.12 | 0.17 | * | * | * | * |
| $P_2O_5$ | 0.26 | 0.3 | 0.32 | 0.24 | 0.34 | 0.34 | 0.38 | 0.28 |
| CaO | 5.61 | 6.02 | 0.53 | 0.32 | 5.92 | 0.36 | 0.57 | 0.32 |
| $Mn_3O_4$ | 0.04 | 0.04 | 0.01 | 0 | 0.04 | 0.04 | 0.01 | 0.01 |
| MgO | 1.94 | 2.14 | 0.35 | 0.29 | 2.14 | 2.33 | 0.43 | 0.38 |
| $SO_3$ | 4.5 | 4.06 | 0.32 | 0.22 | * | * | * | * |
| $Na_2O$ | 0.4 | 0.23 | 0.07 | 0.1 | 0.45 | 0.13 | 0 | 0.07 |
| $K_2O$ | 0.55 | 0.55 | 0.58 | 0.76 | 0.59 | 0.57 | 0.59 | 0.77 |
| Total | | | | | 100 | 100 | 100 | 100 |

**Note:** HUC1 = Highveld coal 1 before sequential leaching test
HLC1 = Highveld coal 1 after sequential leaching test
WL = Water leaching;
AAL …= Ammonium acetate leaching
HClL = Hydrochloric acid leaching
* = BaO, SrO and $SO_3$ were not determined

**Table 4.17:** Inorganic oxide percentages from normalised ICP-OES and XRF analysis of HTA samples of Highveld coal sample 2 (wt %)

| | ICP-OES Data | | | | XRF Data | | | |
|---|---|---|---|---|---|---|---|---|
| | HUC1 | WL HLC1 | AAL HLC1 | HClL HLC1 | HUC1 | WL HLC1 | AAL HLC1 | HClL HLC1 |
| | % | % | % | % | % | % | % | % |
| $SiO_2$ | 46.84 | 48.06 | 56.12 | 64.88 | 45.51 | 46.55 | 56.04 | 64.28 |
| $Al_2O_3$ | 26.22 | 26.44 | 30.64 | 27.41 | 26.19 | 25.94 | 31.56 | 28.13 |
| $Fe_2O_3$ | 4.32 | 4.35 | 4.84 | 4.59 | 4.25 | 4.19 | 4.88 | 4.50 |
| $TiO_2$ | 1.38 | 1.42 | 1.65 | 1.77 | 1.35 | 1.39 | 1.63 | 1.74 |
| BaO | 0.30 | 0.31 | 0.35 | 0.10 | * | * | * | * |
| SrO | 0.47 | 0.47 | 0.38 | 0.06 | * | * | * | * |
| $P_2O_5$ | 0.87 | 0.85 | 1.02 | 0.06 | 0.86 | 0.85 | 1.01 | 0.1 |
| CaO | 9.84 | 10.11 | 2.10 | 0.16 | 9.73 | 9.88 | 2.03 | 0.17 |
| $Mn_3O_4$ | * | * | * | * | 0.06 | 0.06 | 0.03 | 0.01 |
| MgO | 2.80 | 2.86 | 0.87 | 0.25 | 2.80 | 2.83 | 0.84 | 0.29 |
| $SO_3$ | 5.69 | 3.96 | 1.08 | 0.10 | * | * | * | * |
| $Na_2O$ | 0.51 | 0.38 | 0.13 | 0.07 | 0.37 | 0.37 | 0.11 | 0.08 |
| $K_2O$ | 0.70 | 0.73 | 0.80 | 0.56 | 0.68 | 0.71 | 0.79 | 0.57 |

**Note:** HUC2 = Highveld coal 2 before sequential leaching test
HLC2 = Highveld coal 2 after sequential leaching test
WL = Water leaching;
AAL = Ammonium acetate leaching
HClL = Hydrochloric acid leaching
* = $Mn_3O_4$, BaO, SrO and $SO_3$ were not determined

### 4.5.4 Mineralogical analysis of unleached and leached coal particles

Table 4.18 indicates the percentages of the individual minerals in each LTA, based on powder XRD and SIROQUANT evaluation. Figures 4.8-4.9 illustrate the X-ray diffractograms of the LTA from coals 1 and 2 of the feed coal and the residual material from sequential leaching with water, ammonium acetate and hydrochloric acid solutions.

As presented in Table 4.18, feed coals 1 and 2 were found to have 36.4% and 28.4% mineral matter (LTA) respectively. These results are in line with the heat treatment (<400°C) of coal 1; some moisture and volatiles were removed from sample 1 during heat treatment, resulting in an increase in mineral matter content. The feed coal's minerals are primarily made up of kaolinite ($Al_2Si_2O_5(OH)_4$, 52-55%), lesser proportions of quartz ($SiO_2$, 16-26%) and the fluxing elements-bearing mineral dolomite ($CaMg(CO_3)_2$, 8-12%). Minor proportions of the fluxing elements-bearing mineral calcite ($CaCO_3$), illite ($K_{1.5}Al_4(Si_{6.5}Al_{1.5})O_{20}(OH)_4$), the fluxing elements-bearing mineral pyrite ($FeS_2$), the fluxing elements-bearing mineral siderite ($FeCO_3$), the sulphate mineral bassanite

($CaSO_4 \cdot ½H_2O$) and the alumino-phosphate mineral goyazite ($SrAl_3(PO_4)_2(OH)_5.H_2O$) are present. A small proportion of rutile ($TiO_2$) was also present in the LTA samples of these coals.

The silicate and carbonate minerals dominate in the feed coals and their mineral assemblage is consistent with similar data obtained from the analysis of other South African coals (Pinetown et al., 2007).

In coal 1, the quartz content slightly increased after the ammonium acetate leaching stage (from 23.5 to 26.3%) and the kaolinite content slightly increased after the ammonium acetate (from 52.6 to 60.9%) and hydrochloric acid leaching stages (from 60.9 to 68.9%). An increase in the moisture content from 3.3% after water leaching, to 4.0% after the ammonium acetate leaching stage was observed. The results of coal 2 indicated that an outlier (3.0%) in the rutile content in the residual coal particles after the water leaching stage was most probably due to an analytical error. A slight increase in the volatile matter content in coal 2 from 19.3 to 19.5% after the acid leaching, may account for the increased quartz content (from 21.2 to 27.8%) after the acid leaching stage and increased kaolinite content (from 49.6 to 64.5%) after the ammonium acetate leaching stage.

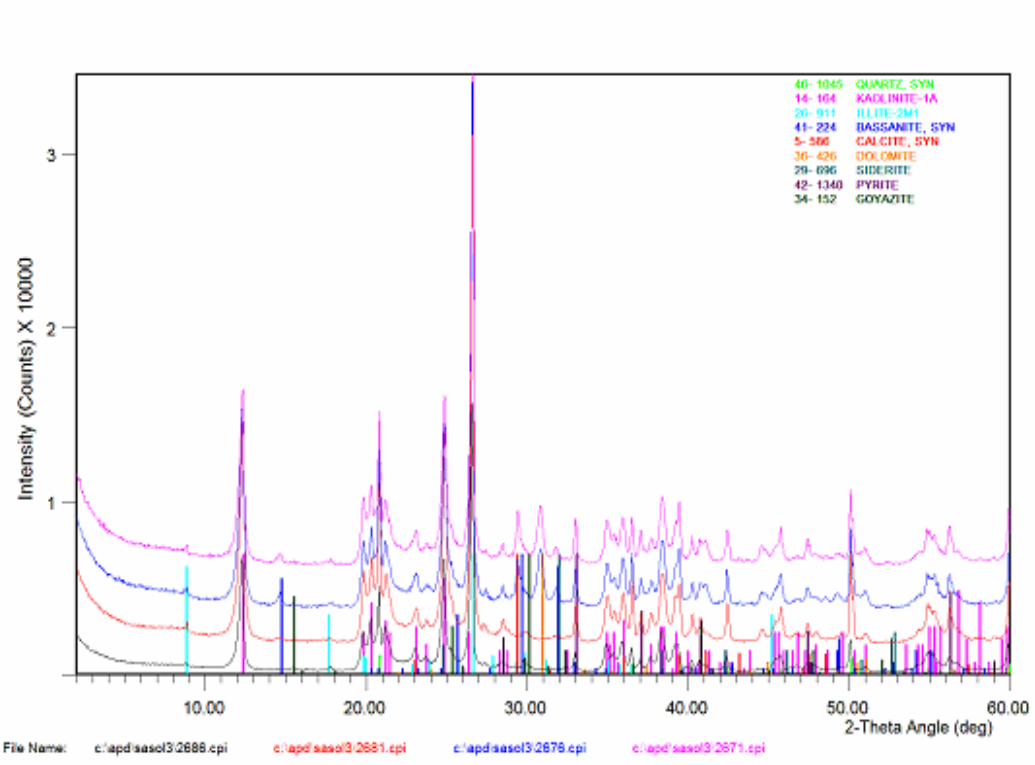


**Figure 4.8**: X-ray diffractograms of LTA from Sample 1 Feed coal (top) to water, ammonium acetate and HCl leaching (bottom).

**Table 4.18**: Mineralogical analysis data for coal LTA samples (wt% of LTA)

| Sample | | *LTA* | Qtz | Kaolin | Illite | I/S | Cal'ite | Dol'it-e | Sid'ite | Pyrite | Rutile | Goy't-e | Bas'te |
|---|---|---|---|---|---|---|---|---|---|---|---|---|---|
| 1 | Feed | 36.4 | 25.7 | 52.9 | 3.0 | | 2.3 | 8.3 | 0.5 | 4.8 | 0.6 | | 1.8 |
| | WL | 36.0 | 23.5 | 52,6 | 3.7 | | 1.3 | 8.8 | 1.1 | 4.1 | 0.7 | | 4.2 |
| | AAL | 31.9 | 26.3 | 60.9 | 2.9 | 4.7 | | | | 4.4 | 0.8 | | |
| | HClL | 23.9 | 22.7 | 68.9 | 2.6 | | | | | 3.5 | 0.9 | 1.5 | |
| 2 | Feed | 28.4 | 16.1 | 54.4 | 3.5 | | 3.8 | 11.4 | 2.1 | 3.5 | 0.7 | 2.4 | 2.1 |
| | WL | 30.8 | 18.2 | 49.6 | 3.7 | | 5.2 | 12.0 | 0.7 | 2.9 | 3.0 | 1.7 | 3.0 |
| | AAL | 26.3 | 21.2 | 64.5 | 3.6 | | | 1.0 | 1.2 | 3.2 | 0.9 | 2.1 | 2.2 |
| | HClL | 29.5 | 27.8 | 61.2 | 2.0 | 4.6 | | | | 3.5 | 0.8 | | |

**Note**: WL= water leaching; AAL =ammonium acetate leaching and HClL = hydrochloric acid leaching
Qtz =Quartz; Kaolin = Kaolinite; I/S = Illite/smectite; Cal'ite= Calcite; Dol'ite = Dolomite;
Sid'ite = Siderite;
Goy'te=Goyazite;..Bas'te=Bassanite;

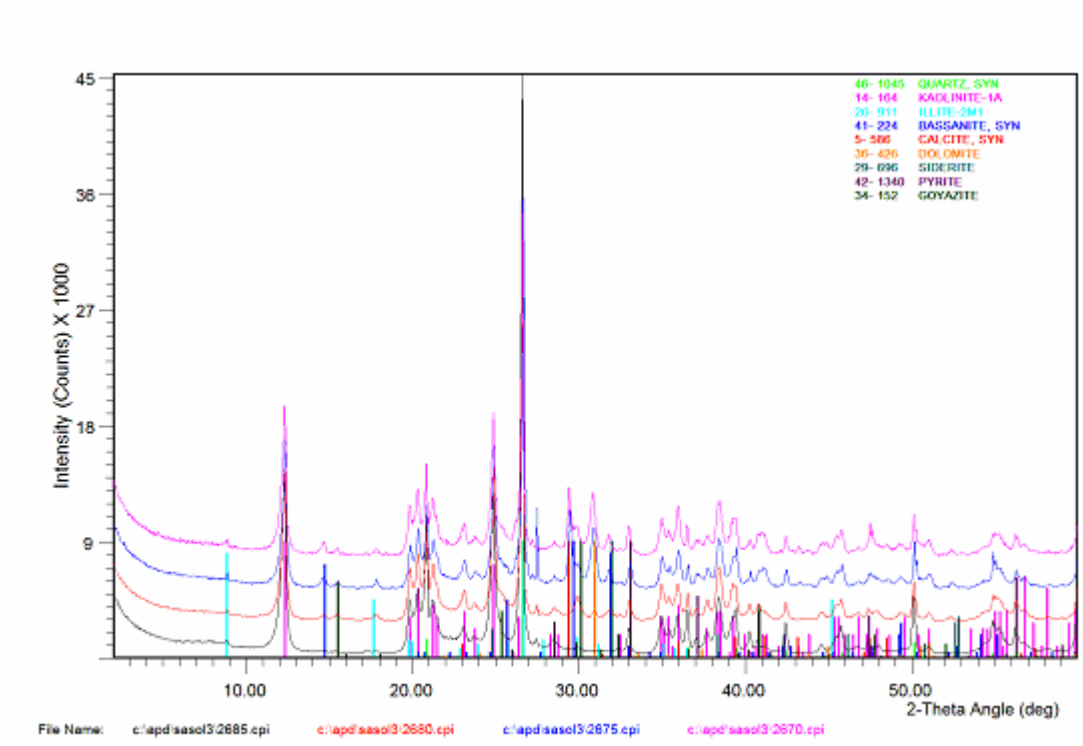


**Figure 4.9**: X-ray diffractograms of LTA from Sample 2 Feed coal (top) to water, ammonium acetate and HCl leaching (bottom).

### 4.5.5 Water leaching

Table 4.14 shows that water leaching reduced the ash yield of HUC1 by 1.2% and that of HUC2 by 0.3%. The primary non-mineral inorganic element found in the leachate of the SAMB coals was Na, along with minor proportions of Ca, K, Mg and Si (Table 4.19). The dissolution of sodium, calcium, potassium, silicon and magnesium in distilled water used as the lixiviant during the sequential leaching step testing, implies that most of the sodium ions dissolved in the pore water within the coal. These results are in line with the previous results (Ward, 1991; Govender, 2005). Cr, Mn, Fe, Al, V and Ti were found not to be present in the leach liquor after water leaching. The pH of the slurry and leachate, before and after leaching, did not differ for these samples evaluated by CHF in this study. This implies that iron-containing minerals such as pyrite and siderite in the coal tested were not partially oxidised.

### 4.5.6 Ammonium acetate leaching

From the results for the coal samples, before and after sequential leaching, given in Table 4.14 it can be seen that subsequent to water leaching, ammonium acetate leaching further reduced the ash yield of coal 1 by 2.0% and that of coal 2 by 2.1%. The leach liquors produced from the sequential leaching of the residual coal particles, after the water leaching with ammonium acetate solution, contained a significantly higher concentration of Ca and to a lesser extent Mg, Na, K, Mn and Si (Table 4.19). The pH values of the leach liquors produced from ammonium acetate leaching of these two coals, slightly increased from the pH value of 7.00 to 7.40, perhaps because of the presence of alkali elements (K and Na) as well as Ca in the leach liquors. Benson and Holm (1985) and Benson (1987) also found that significant amounts of Ca, Mg and Na present in the lignite samples dissolved in ammonium acetate solution during leaching experiments and the researcher suggested that these elements occur mostly in ion-exchangeable form (salts of organic acids in the coal). The elements removed by ammonium acetate leaching are likely to be present in the coal as the salts of carboxylic acid groups.

### 4.5.7 Hydrochloric acid leaching

The acid leaching step further reduced the ash yield of the residual leached coal particles of coal 1 by 1.5% and of the residual leached coal particles of coal 2 by 2.1% (Table 4.14) removing much more of Cr, K, Fe, Al, V, Ti and Si than the previous lixiviants (Table 4.19). Trace amounts of the remaining Mg, Na and Ca were also removed from the residual coal particles by hydrochloric acid leaching. Some of these elements could be derived from sub-

micron illite, illite/smectite, sub-micron clay and carbonate minerals that were removed during the HCl leaching step.

Miller and Given (1978), Benson and Holm (1985), Ward (1991) and Benson (1987) found in their studies that the HCl leaching stage, the last step of CHF, significantly removes elements that are present in the coal in the form of carbonates, hydroxides, oxides and organically-coordinated species. Contrary to the previous results for lignite coal samples that were found by Miller and Given (1978), Benson and Holm (1985), Ward (1991) and Benson (1987), trace proportions of Si, Al, V and Ti dissolved in hydrochloric acid during sequential leaching of Highveld coals. These elements could be derived from the sub-micron clays containing trace amounts of Ti and V, which were removed during the HCl leaching step.

**Table 4.19:** Concentration of elements detected in the leachate of coal samples that were subjected to sequential leaching (ppm) with water, ammonium acetate and hydrochloric acid

| Sample | Lixiviant | Al | Ca | Fe | Cr | Mg | Na | K | Si | Mn | Ti | V |
|---|---|---|---|---|---|---|---|---|---|---|---|---|
| *1* | $H_2O$ | 0 | 62 | 0 | 0 | 13 | 61 | 4 | 2 | 0 | 0 | 0 |
| | $NH_4OAc1$ | 0 | 1886 | 0 | 0 | 188 | 138 | 19 | 2 | 4 | 0 | 0 |
| | $NH_4OAc2$ | 0 | 2786 | 0 | 0 | 869 | 16 | 4 | 4 | 14 | 0 | 0 |
| | $NH_4OAc3$ | 0 | 433 | 0 | 0 | 122 | 5 | 2 | 5 | 4 | 0 | 0 |
| | HCl1 | 819 | 492 | 677 | 17 | 46 | 22 | 54 | 227 | 6 | 1 | 2 |
| | HCl2 | 651 | 36 | 23 | 9 | 13 | 13 | 61 | 11 | 1 | 2 | 1 |
| *2* | $H_2O$ | 0 | 26 | 0 | 0 | 5 | 123 | 6 | 2 | 0 | 0 | 0 |
| | $NH_4OAc1$ | 0 | 3000 | 0 | 0 | 587 | 128 | 25 | 3 | 13 | 0 | 0 |
| | $NH_4OAc2$ | 0 | 1398 | 2 | 0 | 590 | 12 | 3 | 2 | 7 | 0 | 1 |
| | $NH_4OAc3$ | 0 | 349 | 0 | 0 | 143 | 7 | 2 | 4 | 4 | 0 | 0 |
| | HCl1 | 769 | 261 | 828 | 13 | 45 | 11 | 33 | 152 | 6 | 0 | 2 |
| | HCl2 | 456 | 21 | 200 | 1 | 14 | 7 | 31 | 161 | 0 | 0 | 0 |

**Note:** L1= leach liquor produced after sequential leaching of HUC1
L2 = leach liquor produced after sequential leaching of HUC2
$NH_4OAc1$, $NH_4OAc2$, $NH_4OAc3$ = Ammonium acetate leaching steps 1, 2 and 3
HCl1, HCl2 = Hydrochloric acid leaching steps 1 and 2.

### 4.5.8 Physical analysis:Ash Fusion Temperatures (AFT)

The ash fusion temperatures of the Higveld coal samples, as expressed by the initial deformation temperatures, varied from 1150 to >1500°C (Table 4.20) with flow temperatures being 40 to 110°C higher. From the results given in Table 4.20, it is clear that the AFT values of these coals remained constant before and after the water leaching step. The AFT values increased to >1500°C after the ammonium acetate and hydrochloric acid leaching steps, related to the loss of fluxing elements (such as Ca, Mg and Fe) (Table 4.16 and Table 4.17) and the removal of carbonates (calcite, dolomite and siderite) as shown by XRD data (Table

4.18). Electron microprobe analyses of macerals from similar coals (Table 4.12) suggest that Ca, Al and possibly Mg may also occur as inherent components of the individual macerals and these might also have been removed by ammonium acetate and acid treatment. Such observations are in agreement with those of Van Dyk et al. (2005), who suggested that acid leaching removes potentially harmful minerals from the coal, leading to a rapid increase in the ash fusion temperatures.

**Table 4.20**: AFT's (°C) of the feed coal and residual coal particles after sequential leaching with water, ammonium acetate and hydrochloric acid

| Lixiviants | Samples | ID | ST | HT | FT |
|---|---|---|---|---|---|
| Sample 1 | HUC | 1310 | 1320 | 1330 | 1350 |
| | $H_2O$ | 1310 | 1320 | 1330 | 1340 |
| | $NH_4OAc$ | >1550 | >1550 | >1550 | >1550 |
| | HCl | >1550 | >1550 | >1550 | >1550 |
| Sample 2 | HUC | 1320 | 1360 | 1390 | 1430 |
| | $H_2O$ | 1340 | 1360 | 1390 | 1430 |
| | $NH_4OAc$ | >1550 | >1550 | >1550 | >1550 |
| | HCl | >1550 | >1550 | >1550 | >1550 |

**Note:** HUC1 and HUC2 = Highveld coal 1 and Highveld coal 2 before sequential leaching test
HLC1 and HLC2 = Highveld coal 1 and Highveld coal 2 after sequential leaching test
ID = Initial deformation temperature,
ST = Spherical temperature
HT = Hemispherical temperature,
FT = Flow temperature

The relationship of these changes in mineralogy and chemistry to the ash fusion characteristics is illustrated in Figure 4.10, where the initial deformation temperatures after each treatment are seen to be inversely related for each coal to the total proportions of CaO, MgO and $Fe_2O_3$ in the ashes of the relevant coal residues.

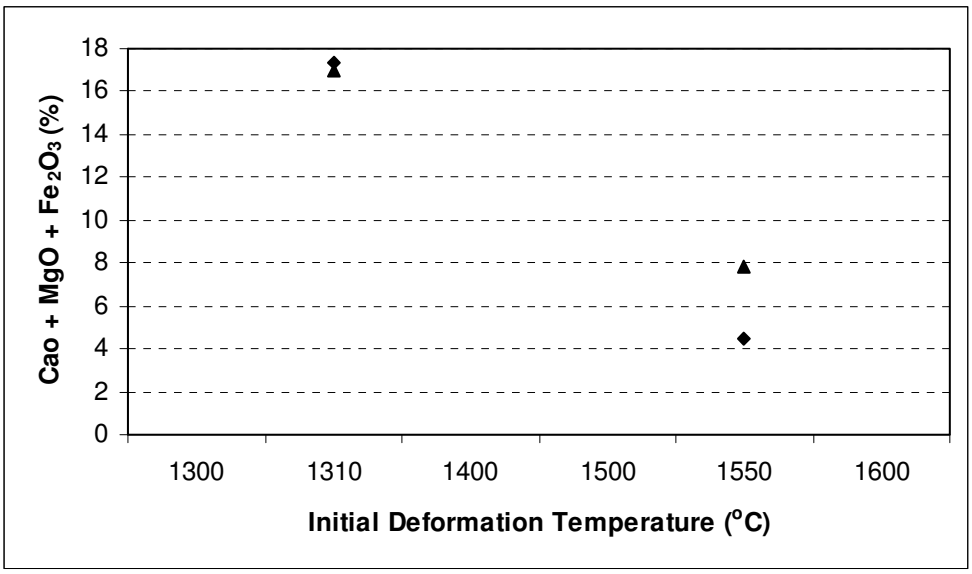


**Figure 4.10:** Relation between deformation temperature and proportion of CaO, MgO and $Fe_2O_3$ in coal ashes after each leaching process. Sample with deformation temperatures >1550ºC have been plotted at 1550ºC (from ICP data).

## 4.6 Distribution of inorganic elements in the minerals and macerals

The CCSEM results (Table 4.12) Petrography analysis (Table 4.4) and Electron microprobe results (Table 4.12), were used to calculate amounts of inorganic elements in the minerals and macerals present in the coals analysed in this study. Appendix F (Table F1) shows calculated total amounts of inorganic elements from minerals present in the Highveld coals obtained when using CCSEM analysis of coals. It can be seen from the results given in Table F2 that significantly higher amounts of Al, Si, Ca and Fe and to a lesser extent Ti, P, Mg and K are contained in the minerals present in the coals. As expected, small amounts of C and H are contained in the minerals in the coal. Nitrogen was not found to be present in the coal minerals.

From the results given in Table F1 it is clear that macerals in the coal contain small amounts of Mg, Al, Si, S, Ca and Ti. Macerals in the coals evaluated in this study contain about 0.4-1% organically-bound inorganic elements (Mg, Al, Si, S, Ca and Ti). Table F2 shows calculated concentrations of inorganic elements in the minerals present in Highveld coals, and Table F1 indicates calculated concentrations of the organic elements and inorganic elements in all coal macerals (the concentrations of elements in these two tables total 100%). As expected, significant amounts of C, H, N and O are reported to the organic matter (macerals). Some of these inorganic elements can interact with each other at elevated temperatures and

pressures and subsequently volatilise in the form of gases during coal pyrolysis. Whereas other inorganic elements in the macerals, as well as fluxing inorganic elements from mineral associations in the coal, could significantly contribute to sintering and slagging of mineral matter at elevated temperatures during coal gasification.

# CHAPTER 5
# RESULTS AND DISCUSSION - COAL SIZE AND DENSITY FRACTIONS ANALYSES

In this chapter the analytical results for coal size and density fractions produced from the feed coal are presented and discussed.

## 5.1 Characterisation of coal size fractions of feed coal by chemical analyses

### 5.1.1 Ultimate analysis of coal size fractions

Table 5.1 shows that the proportion of carbon varies between 77.02-80.12% as the size of coal particles decrease from -53+26.2mm to -4mm. The results for the coal size fractions also reveal that there are slight variations in proportions of hydrogen and nitrogen. Interestingly, the -75+53mm fraction contains high concentration of the total sulphur and to a lesser extent in the -53+26mm size fraction**.**

**Table 5.1:** The ultimate analysis of coal size fractions feed coal (dry, ash-free basis) (wt%)

| **Coal size fractions** | **-75 +53mm** | **-53 +26.2mm** | **-26.2 +13.2mm** | **-13.2 +9.5mm** | **-9.5 +6.7mm** | **-6.7+ 4.7mm** | **-4.7 +4mm** | **-4mm** |
|---|---|---|---|---|---|---|---|---|
| Carbon (%) | 78.14 | 78.65 | 79.57 | 80.12 | 80.38 | 79.90 | 77.02 | 80.03 |
| Hydrogen (%) | 3.72 | 4.06 | 4.04 | 4.00 | 3.89 | 4.00 | 4.04 | 3.98 |
| Nitrogen (%) | 2.06 | 2.10 | 2.14 | 2.14 | 2.10 | 2.08 | 2.14 | 2.15 |
| Total sulphur (%) | 4.58 | 1.84 | 1.22 | 0.99 | 1.18 | 1.21 | 1.01 | 1.00 |
| Oxygen (%) by difference. | 11.49 | 13.35 | 13.03 | 12.74 | 12.45 | 12.81 | 15.79 | 12.84 |

### 5.1.2 Proximate analysis of coal size fractions

In contrast, Table 5.2 shows that there is no notable difference in concentrations of inherent moisture, ash, volatile matter and fixed carbon in the coal size fractions analysed in this study.

**Table 5.2:** The proximate analysis of coal size fractions

| Coal size fractions | -75 +53mm | -53 +26.2 | -26.2 +13.2mm | -13.2 +9.5mm | -9.5 +6.7mm | -6.7+ 4.7mm | -4.7 +4mm | -4mm |
|---|---|---|---|---|---|---|---|---|
| IM (%) | 4.6 | 4.4 | 4.9 | 4.9 | 4.8 | 4.7 | 4.8 | 4.7 |
| Ash (%) | 26.4 | 28.9 | 23.8 | 23.4 | 24.7 | 23.3 | 24.1 | 22.7 |
| VM (%) | 22.1 | 21.2 | 21.6 | 21.2 | 21.2 | 21.3 | 21.3 | 22.0 |
| FC (%) | 46.9 | 45.5 | 49.7 | 50.5 | 49.3 | 50.7 | 49.8 | 50.6 |

The XRF analysis (Table 5.3) indicates that the coarser fraction (-75+53mm) contains a higher proportion of sulphur (in line with Table 5.1) and to a lesser extent in the -53+26mm size fraction in comparison with other coal size fractions analysed in this study. The significantly higher sulphur proportion in the -75+53mm and -53+26mm size fractions is associated with a high Fe content (Table 5.3), indicating that pyrite is concentrated in these two coarse coal size fractions. Similarly, other fluxing elements such as Ca and Mg are concentrated in the -75+53mm fraction. The presence of these fluxing elements in this coal size fraction can be expected to enhance the sintering and slagging of mineral matter at elevated temperatures and pressures, subsequently resulting in clinker formation during coal gasification/combustion. A high proportion of phosphorus (which could possibly be present as apatite) is also present in the -75+53mm coal size fraction.

**Table 5.3:** Inorganic oxide percentages (wt %) from XRF analysis of coal size fractions

| Coal size fractions | -75 +53mm | -53 +26.2mm | -26.2 +13.2mm | -13.2 +9.5mm | -9.5 +6.7mm | -6.7+ 4.7mm | -4.7 +4mm | -4mm |
|---|---|---|---|---|---|---|---|---|
| $SiO_2$ | 10.90 | 16.20 | 13.40 | 13.60 | 13.70 | 12.60 | 13.00 | 11.50 |
| $Al_2O_3$ | 4.90 | 6.90 | 6.60 | 7.10 | 6.80 | 6.50 | 6.80 | 6.60 |
| $Fe_2O_3$ | 3.93 | 1.61 | 1.07 | 0.95 | 0.87 | 0.79 | 0.81 | 0.86 |
| $TiO_2$ | 0.23 | 0.41 | 0.38 | 0.38 | 0.39 | 0.36 | 0.38 | 0.35 |
| $P_2O_5$ | 0.89 | 0.17 | 0.22 | 0.24 | 0.27 | 0.26 | 0.26 | 0.26 |
| CaO | 4.68 | 2.66 | 2.00 | 1.87 | 1.87 | 1.87 | 1.90 | 2.12 |
| MgO | 1.20 | 0.80 | 0.80 | 0.80 | 0.50 | 0.50 | 0.50 | 0.50 |
| $Na_2O$ | 0.02 | 0.05 | 0.04 | 0.07 | 0.04 | 0.04 | 0.04 | 0.05 |
| $K_2O$ | 0.19 | 0.30 | 0.24 | 0.25 | 0.25 | 0.24 | 0.24 | 0.23 |
| $SO_3$ | 3.05 | 1.27 | 0.94 | 0.82 | 0.72 | 0.70 | 0.62 | 0.53 |

## 5.2 Mineralogical analysis of coal size fractions

### 5.2.1 CCSEM analysis of coal size fractions

Figure 5.1 illustrates back-scattered electron images with the prominent differences between the eight size fractions that were crushed before analysis. The appearance of the carbon-rich organic phase in these back-scattered electron images (with atomic number contrast) is black to dark grey and minerals are light grey to white.

The results in Figure 5.1 also show that, with exception of the -75+53mm size fraction, the remaining size fractions contain similar minerals. However, the -75+53mm size fraction has a higher proportion of pyrite associated with coarse-grained sandstone, coarse pyrite cleat fragments and coarse calcite cleat fragments. The characteristics of selected particles of coal and rock fragments shown in Figure 5.1, are described as follows:

- Particle 1 - pyrite (white) is associated with coarse grained quartz-rich (grey) sandstone;
- Particle 2 - coarse calcite cleat (grey) is associated with organic fraction;
- Particle 3 - fine-grained kaolinite and quartz siltstone rock fragment;
- Particle 4 - coarse grained quartz rich sandstone rock fragment;
- Particle 5 - fine calcite/dolomite (grey) cleats transecting carbon matrix (black);
- Particle 6 - kaolinite-rich (grey) mudstone rock fragment, included microcline and muscovite (elongated grain) minerals are present;
- Particle 7 - coarse microcline-rich fragment;
- Particle 8 - complex intergrowth of calcite/dolomite in a carbon-rich matrix (black);
- Particle 9 - large predominantly dolomite (grey) inclusions in carbon-rich matrix (black);
- Particle 10 - medium grained sandstone rock fragment with equal proportions of kaolinite (grey), quartz (light grey) and minor proportions of microcline (white).

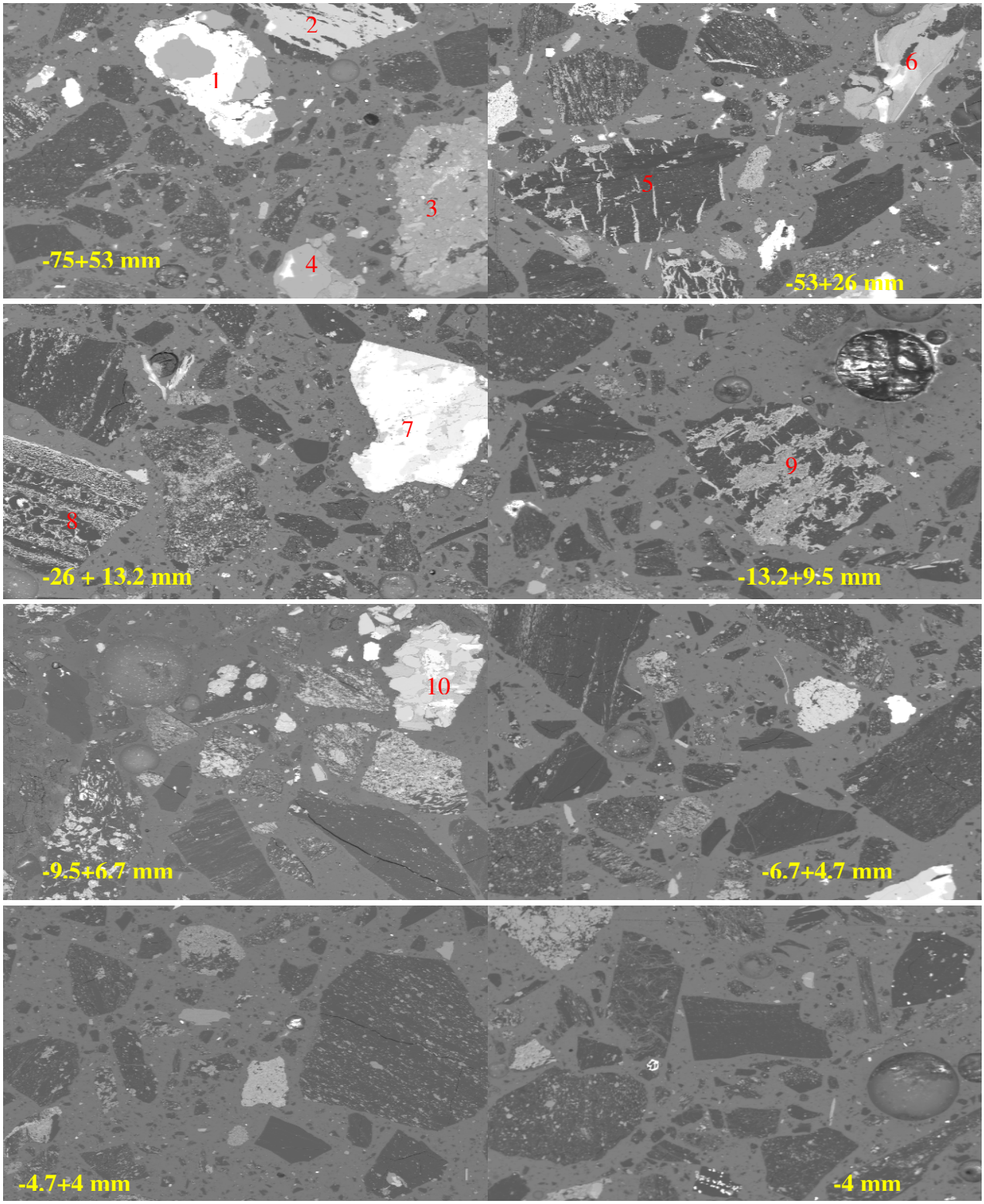


**Figure 5.1:** Back-scattered electron images of the eight size fractions. The particle characteristics and variation in proportions of minerals are illustrated. The width of the each image field is approximately 6.3 mm.

### a) Concentrations of minerals in coal size fractions (mass-%)

The CCSEM technique was used to determine concentrations of minerals present in the individual coal size fractions. The calculated mass-% mineral distribution is summarised in Table 5.4. The results given in Table 5.4 confirm that the -75+53mm size fraction contained significantly higher proportions of fluxing elements-bearing minerals such as pyrite, dolomite and calcite and a corresponding low proportion of kaolinite (in line with the XRF results in Table 5.3). The apatite mineral, which could also play a significant role to lower the ash fusion temperature of mineral matter at elevated temperatures, concentrated in the coarse coal fraction (the-75+53mm size fraction). High concentrations of the carbonate minerals, as well as pyrite in the sink fraction (<1.8g/cm$^3$) that were also detected by CCSEM, corroborated these results (Table 4.11). Quartz was also found to be somewhat concentrated in the coarse coal particles and remained fairly constant as the coal fractions decreased from the -26.2+13.2mm to-4.7+4mm in comparison with other coal fractions analysed in this study. This favourably corresponds to the observed variations in $Al_2O_3$, $SiO_2$, $Fe_2O_3$, CaO and MgO contents (Table 5.3).

**Table 5.4:** Mineral proportions for the individual size fractions (mass-%)

| **Coal size fractions** | **-75 +53mm** | **-53 +26.2mm** | **-26.2 +13.2mm** | **-13.2 +9.5mm** | **-9.5 +6.7mm** | **-6.7+ 4.7mm** | **-4.7 +4mm** | **-4mm** |
|---|---|---|---|---|---|---|---|---|
| Pyrite | 6.2 | 1.7 | 1.9 | 1.1 | 1.5 | 0.9 | 0.9 | 1.4 |
| Quartz | 7.2 | 9.6 | 5.2 | 6.9 | 6.2 | 5.2 | 5.9 | 4.8 |
| Microcline | 0.8 | 0.8 | 0.6 | 0.5 | 0.5 | 0.2 | 0.3 | 0.2 |
| Muscovite/ Illite | 1.0 | 2.3 | 1.2 | 4.5 | 1.8 | 1.0 | 1.6 | 1.0 |
| Kaolinite | 8.1 | 15.7 | 14.4 | 11.6 | 13.6 | 14.8 | 15.5 | 13.6 |
| Anatase | 0.1 | 0.2 | 0.1 | 0.1 | 0.1 | 0.1 | 0.2 | 0.2 |
| Ankerite | 0.1 | 0.1 | 0.1 | 0.1 | 0.1 | 0.1 | 0.1 | 0.1 |
| Siderite | 0.1 | 0.1 | 0.0 | 0.0 | 0.0 | 0.0 | 0.0 | 0.2 |
| Calcite | 5.2 | 3.2 | 1.9 | 1.8 | 1.8 | 1.8 | 2.1 | 3.1 |
| Dolomite | 4.4 | 4.0 | 2.8 | 2.9 | 2.9 | 2.7 | 3.1 | 2.1 |
| Apatite | 0.9 | 0.0 | 0.4 | 0.2 | 0.2 | 0.1 | 0.2 | 0.1 |
| Other | 0.6 | 0.4 | 0.3 | 0.6 | 0.7 | 0.2 | 0.4 | 0.2 |
| Coal (carbon)# | 65.3 | 61.7 | 71.0 | 69.7 | 70.6 | 72.9 | 69.9 | 73.1 |

Table 5.5 illustrates the mineral distribution across the individual size fractions. The mineral distribution across the individual size fraction was calculated by using the proportion of mineral in the individual size fraction (Table 5.4) and the calculated mass-% size distribution (mass retained) in Figure 3.2. The individual mineral distributions were compared with the mass-% distribution across the size fractions or particle size distributions (PSD). The results indicated that a comparatively high proportion of pyrite (25.6%) and to a lesser extent calcite (16.9%) and dolomite (11.3%) are concentrated in the -75+53mm size fraction. The -26.2+13.2mm size fraction contains a high proportion of other minerals, along with low proportions of quartz and muscovite/illite. As the size of coal particles decreases from the -13.2+9.5mm to -4.7+4mm, proportions of other minerals, and carbon also decrease, with the exception of kaolinite.

**Table 5.5:** Percent mineral distribution across size fractions (wt%)

| **Coal size fractions** | **-75 +53mm** | **-53 +26.2mm** | **-26.2 +13mm** | **-13.2 +9.5mm** | **-9.5 +6.7mm** | **-6.7 +4.7mm** | **-4.7 +4mm** | **-4mm** |
|---|---|---|---|---|---|---|---|---|
| Pyrite | 25.60 | 17.80 | 34.50 | 6.50 | 8.00 | 3.00 | 1.00 | 3.60 |
| Calcite | 16.90 | 26.60 | 27.50 | 8.50 | 7.70 | 4.50 | 2.00 | 6.30 |
| Dolomite | 11.30 | 26.20 | 30.50 | 11.00 | 9.80 | 5.30 | 2.30 | 3.50 |
| Kaolinite | 4.80 | 23.40 | 36.80 | 10.00 | 10.50 | 6.80 | 2.70 | 5.00 |
| Quartz | 8.90 | 29.90 | 27.90 | 12.40 | 10.00 | 5.00 | 2.10 | 3.70 |
| Microcline | 10.70 | 28.50 | 37.30 | 9.60 | 8.90 | 2.50 | 1.10 | 1.50 |
| Muscovite/ illite | 4.20 | 25.50 | 23.30 | 28.80 | 10.10 | 3.30 | 2.00 | 2.90 |
| Coal (carbon)# | 7.70 | 18.40 | 36.30 | 12.10 | 10.90 | 6.70 | 2.40 | 5.40 |

**Note:** #Coal-refers the carbon-rich matrix and represents the macerals

### b) Characterisation of particles of the screened coal fractions

To determine proportions of extraneous mineral matter, as well as the included mineral matter (mineral matter that is associated with the carbon matrix or present in the coal macerals), the same back-scattered electron images of particles taken during the CCSEM analysis of coal fractions were used to classify particles into the different texture groups described in Figures 3.8-3.9. The area-% proportions of these particle types are summarised in Table 5.6 and percent distribution across the size fractions in Table 5.5.

From the results given in Table 5.6, it can be seen that the proportion of included minerals slightly increased with a decrease in the coal size fractions. The -75+53mm size fraction contains comparatively higher proportions of sandstone rock fragment, pyrite cleats, carbonate cleats and a smaller proportion of siltstone/mudstone rock fragment in comparison with other coal size fractions analysed in this study.

**Table 5.6:** Area-% proportions of the major particle types

| **Coal size fractions** | **-75 +53mm** | **-53 +26.2mm** | **-26.2 +13mm** | **-13.2 +9.5mm** | **-9.5 +6.7mm** | **-6.7 +4.7mm** | **-4.7 +4mm** | **-4mm** |
|---|---|---|---|---|---|---|---|---|
| Coal rich particles (MM <60 vol-%) | 76.80 | 73.60 | 85.20 | 86.30 | 83.50 | 92.50 | 91.90 | 92.90 |
| Siltstone/ mudstone rock fragment | 2.90 | 16.00 | 10.00 | 11.10 | 10.90 | 6.30 | 5.80 | 4.30 |
| Sandstone rock fragment | 8.90 | 7.90 | 2.00 | 1.20 | 3.70 | 0.50 | 1.10 | 0.90 |
| Pyrite cleats | 5.90 | 2.20 | 0.60 | 0.20 | 0.20 | 0.00 | 0.10 | 0.10 |
| Carbonate cleats | 3.00 | 0.10 | 2.00 | 1.00 | 1.00 | 0.40 | 1.00 | 1.80 |
| Carbonate and pyrite cleats | 2.50 | 0.00 | 0.00 | 0.10 | 0.50 | 0.20 | 0.00 | 0.00 |
| Kaolinite and pyrite cell cavities | 0.00 | 0.10 | 0.20 | 0.00 | 0.10 | 0.10 | 0.00 | 0.10 |

Table 5.7 shows that the -75+53mm coal fraction contains a low proportion of the carbon-rich particles and a marginally higher proportion of the extraneous carbonate and pyrite cleats. Interestingly, pyrite and kaolinite cell cavities were not contained in this coal fraction, but significantly higher proportions of pyrite and kaolinite cell cavities (23.50% and 57.80% of the total) were found in the -53+26mm and -26+13.2mm size fractions respectively. The

absence of the pyrite and kaolinite cell cavities in the -75+53mm coal fraction could imply that this fraction may contribute little to the sintering and slagging of mineral matter during coal gasification or combustion.

High proportions of the siltstone/mudstone rock fragments (32% and 34% of the total) are contained in the two largest fractions (-75+53mm and -53+26mm). In excess of 40% of the sandstone is in the -53+26mm size fraction. Significantly higher proportions (39.70% and 38.40%) of the extraneous pyrite cleat fragments are in the -53+26mm and -75+53mm size fractions respectively, when compared to other coal size fractions analysed in this study. The results from Table 5.7 also reveal that a substantially higher proportion of the carbonate cleat fragments (52%) are concentrated in the -26+13.2mm size fraction, when compared to other size fractions analysed.

**Table 5.7:** Percent particle type distribution across size fractions

| **Coal size fractions** | **-75 +53mm** | **-53 +26.2mm** | **-26.2 +13mm** | **-13.2 +9.5mm** | **-9.5 +6.7mm** | **-6.7 +4.7mm** | **-4.7 +4mm** | **-4mm** |
|---|---|---|---|---|---|---|---|---|
| Coal-rich particles (MM <60 vol-%) | 7.50 | 18.20 | 36.00 | 12.30 | 10.60 | 7.10 | 2.60 | 5.70 |
| Siltstone /mudstone rock fragment | 2.30 | 32.00 | 34.20 | 12.90 | 11.20 | 3.90 | 1.30 | 2.20 |
| Sandstone rock fragment | 19.50 | 43.80 | 19.30 | 3.90 | 10.70 | 0.90 | 0.70 | 1.20 |
| Pyrite cleats | 39.70 | 38.40 | 17.40 | 2.00 | 2.00 | 0.10 | 0.20 | 0.20 |
| Carbonate cleats | 18.00 | 2.00 | 52.40 | 9.10 | 8.00 | 2.00 | 1.80 | 6.80 |
| Carbonate and pyrite cleats | 71.50 | 2.80 | 0.0 | 3.30 | 19.00 | 3.30 | 0.00 | 0.00 |
| Kaolinite and pyrite cell cavities | 0.00 | 23.50 | 57.80 | 0.0 | 9.40 | 3.60 | 0.90 | 4.80 |

### c) Liberation characteristics of minerals of the screened coal fractions

In order to describe the liberation characteristics of minerals in the coal size fractions, all coal size fractions produced by dry screening (excluding the -4.7+4mm size fraction) were ground to 100% passing 1mm. A sample of the -4.7+4mm size fraction was pulverised to 100% passing 212µm. As expected, pulverising coal samples should technically liberate mineral matter that is associated within the carbon matrix (coal macerals). The CCSEM and QEMSCAN analyses of coal revealed that the average size of mineral grains in South African coals is less than 20µm. In order to obtain 100% mineral liberation during coal pulverising, the coal must be pulverised to 100% passing 20µm. To minimise the impact of excessive pulverising only the coarse particles are included in the CCSEM liberation analysis. The results from the minerals' liberation study can provide the proportions of the included minerals that are presumed to be responsible for the initiation of the melting of mineral matter under reducing and oxidising conditions during coal combustion or gasification. Partially excluded mineral particles could presumably attach to the melt and form small and large clinkers in the gasifier.

In this study the liberation groups are defined as follows:

- Included liberation group – mineral matter proportion is less than 20 vol.-percent and the organic coal fraction exceeds 80 vol.-percent;
- Middling liberation group – mineral matter proportion is between 20 to 60 vol.-percent and organic coal fraction is between 40-80 vol.-percent. This is analogous to the carbominerite microlithotype group;
- Extraneous liberation group – mineral matter proportion exceeds 60 vol.-percent and proportion of organic coal fraction is less than 40 vol.-percent. This is analogous to the minerite microlithotype group.

CCSEM analysis shows on average that (based on their minerals) 61.5 mass-percent of the coal particles in the coal samples are classified as "included", 22.0 mass-percent are "middlings" and 16.6 mass-percent are "extraneous". In addition, the results reveal that the majority of minerals (about 50.8%) in the coal sample are present as "extraneous" particles, while the remaining mineral particles (49.2%) occur as "middling" and "included" particles. The proportions of particles produced during the pulverising of the different coal size fractions, as well as the percent mineral proportion for each liberation group, are depicted in

Figures 5.2 and 5.3. Figure 5.2 shows that there is a slight increase in the concentrations of the "included"type particles, with a decrease in the coal size, excluding the -53+26.2mm, 13.2+9.5mm and -9.5+4.7mm size fractions. Excluding the -9.5+4.7mm size fraction, the proportion of extraneous particles gradually decreases with a decrease in the coal size fractions. There is a gradual increase in the proportion of the "included" particles and corresponding decrease in the proportion of "extraneous" particles with a decrease in the size fractions (Figure 5.2). From Figure 5.3 it is clear that a higher proportion (37.8% of total mineral proportions) of the minerals are "extraneous" particles, in the coarser size fractions (>13.2mm), whereas a higher proportion of the minerals are "included" and "middling" particles in the finer size fractions.

Run of mine coal samples consist of coarse "stone" and organic-rich particles with varying proportions of the included minerals. During the mining activities and further sample preparation using physical methods such as screening and crushing, the carbon-rich particles (coal maceral particles), with varying proportions of the included minerals, will possibly break into smaller fragments; whereas, some stones or rock fragments will not readily break into smaller fragments. This is a plausible explanation for the trends observed in Figures 5.2 and 5.3 and the distribution of extraneous rock fragments, pyrite cleat fragments and calcite cleat fragments (Table 5.7).

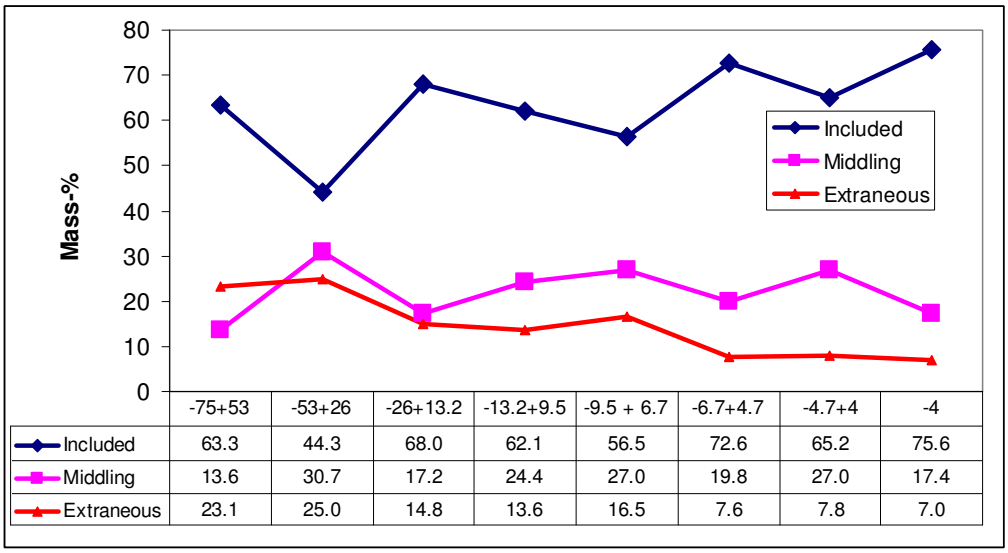


| | -75+53 | -53+26 | -26+13.2 | -13.2+9.5 | -9.5 + 6.7 | -6.7+4.7 | -4.7+4 | -4 |
|---|---|---|---|---|---|---|---|---|
| Included | 63.3 | 44.3 | 68.0 | 62.1 | 56.5 | 72.6 | 65.2 | 75.6 |
| Middling | 13.6 | 30.7 | 17.2 | 24.4 | 27.0 | 19.8 | 27.0 | 17.4 |
| Extraneous | 23.1 | 25.0 | 14.8 | 13.6 | 16.5 | 7.6 | 7.8 | 7.0 |

**Figure 5.2:** Overall particle liberation characteristics.

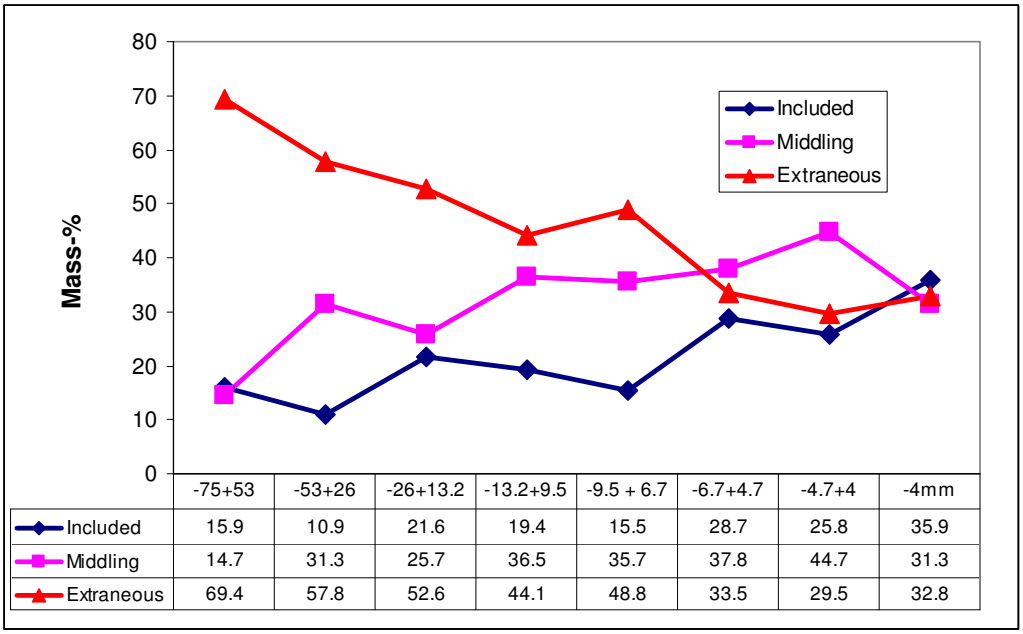


| | -75+53 | -53+26 | -26+13.2 | -13.2+9.5 | -9.5 + 6.7 | -6.7+4.7 | -4.7+4 | -4mm |
|---|---|---|---|---|---|---|---|---|
| Included | 15.9 | 10.9 | 21.6 | 19.4 | 15.5 | 28.7 | 25.8 | 35.9 |
| Middling | 14.7 | 31.3 | 25.7 | 36.5 | 35.7 | 37.8 | 44.7 | 31.3 |
| Extraneous | 69.4 | 57.8 | 52.6 | 44.1 | 48.8 | 33.5 | 29.5 | 32.8 |

**Figure 5.3:** Percent mineral distribution across the different liberation group.

In the same manner, the liberation characteristics of the individual minerals can be determined (Table 5.8). It is interesting to note that 72% of the pyrite present in the coal occurs as extraneous particles, whereas 13.2% and 15.3% of pyrite in the coal are included and middling particles respectively (Table 5.8). In line with this, the CCSEM analysis of coal particles indicates that pyrite predominantly occurs as extraneous coarse cleat fragments and is associated with coarse to medium grained sandstone (Table 5.7). A low proportion of pyrite, which is associated with kaolinite, is present in the coal. A significant proportion of calcite in the coal occurs as coarse calcite-rich cleat fragments; however, the siltstone/mudstone rock fragments contain a large proportion of kaolinite. A low proportion (23.4%) of calcite occurs in the "included" particles, whereas 26.6% of calcite occurs in "middling" particles. From Table 5.8 it can be seen that a small proportion of dolomite in the coal occurs as extraneous particles, whereas dolomite predominantly occurs as included and middling particles. A high proportion (45.7%) of apatite occurs as inclusions in the organic-rich matrix.

A high proportion of quartz (63%), microcline (85%) and muscovite/illite (66%) occur as extraneous particles. This is as expected, since quartz, microcline and muscovite/illite are common constituents of arkosic sandstone rock fragments.

The included minerals (kaolinite/quartz/calcite/dolomite/pyrite) in carbon-rich particles ("included" and "middling") can presumably interact with one another to lower the ash fusion temperature of mineral matter at elevated temperatures and result in slag/clinker formation

during coal gasification or combustion. In addition, the fluxing elements-bearing minerals (pyrite, dolomite and calcite) that are associated with clays (kaolinite, illite) in the rock fragments (sandstone and mudstone/siltstone) can also reduce the ash fusion temperature of mineral matter at elevated temperatures, to form a melt which will presumably result in slag/clinker formation during the heat treatment of coal.

**Table 5.8:** Average liberation characteristics of individual minerals

| Particles | Included | Middling | Extraneous |
|---|---|---|---|
| Pyrite | 13.20 | 15.30 | 71.50 |
| Calcite | 23.40 | 26.60 | 49.90 |
| Dolomite | 44.00 | 43.70 | 12.30 |
| Apatite | 45.70 | 22.10 | 32.20 |
| Kaolinite | 22.50 | 31.00 | 46.50 |
| Quartz | 16.80 | 20.50 | 62.80 |
| Microcline | 4.00 | 11.20 | 84.80 |
| Muscovite/illite | 12.10 | 22.10 | 65.80 |

## 5.3 Characterisation of density coal fractions by analytical techniques

As was stated in the previous section, the coal feedstock to the coal-conversion process, contains minerals that are associated with the carbon matrix and also with the extraneous rock fragments. The proportions of fluxing elements-bearing minerals and organically-bound inorganic elements (that are expected to cause the slagging process during gasification) could significantly depend on particle size, mode of occurrence of mineral matter in the coal and the density of the coal particles. To test this, coal samples were taken from the coal belt of each coal mine using the procedure developed by the operators from the mine. In the experimental procedure a 50kg coal sample was taken from the coal belt every 15min. Approximately 100kg coal sample was separated, using a mixture of tetra-bromo ethane and benzene at a density of 1.8g/cm$^3$ to produce float and sink fractions. The proportions of float and sink fractions were 83-93% and 7-17% respectively.

The sink and float fractions produced in this manner were separately crushed and pulverised to obtain 100% passing 1mm. The prepared samples of the composites from the different mines' float and sink fractions were subsequently submitted for proximate, ultimate,

elemental and ash fusion analyses. The proximate, ultimate and elemental analyses of the float and sink fractions were used to predict the mineral proportions of the calculated feed coal, based on the van Alphen Consultancy Coal Quality Predictor model. The model is also based on the elemental analysis of the mineral matter present in the coal.

### 5.3.1 Petrographic results for float (<1.5g/cm$^3$), middling (1.5-1.8g/cm$^3$) and sink (>1.8g/cm$^3$) fractions

The maceral and microlithotype group analysis results obtained are summarized in Table 5.9 and Table 5.10. The maceral and microlithotype results presented in Tables 5.9 and 5.10 follow the expected trends. The float coal fraction (<1.5g/cm$^3$) contains significantly higher proportions of vitrinite, liptinite, reactive semi-fusinite, inert semi-fusinite+fusinite and sclerotirite in comparison with the sink fraction. Note that the average vitrinite density is 1.3g/cm$^3$, liptinite is 1.25g/cm$^3$ and inertinite is 1.5g/cm$^3$ (Falcon and Snyman, 1986). As expected, significant proportions of mineral matter (quartz, clays, carbonates, pyrite) as stated in (Table 5.10) reported in the sink fraction (>1.8g/cm$^3$).

From the results given in Table 5.10, it is clear that the middling fraction (1.5–1.8g/cm$^3$) contained higher proportions of quartz, clay, carbonates and pyrite minerals in relation to the float fraction (<1.5g/cm$^3$).

**Table 5.9:** Maceral group analysis on coal samples (%vol)

| Density fraction | Vitrinite | Liptinite | RSF | ISF | Fus/Scl | Mic | Inertodet | Qtz/ Cly | Carbs | pyrite | Others |
|---|---|---|---|---|---|---|---|---|---|---|---|
| <1.5g/cm$^3$ | 39.60 | 4.40 | 13.20 | 31.60 | 1.40 | 1.00 | 7.80 | 0.40 | 0.00 | 0.60 | 0.00 |
| 1.5-1.8g/cm$^3$ | 6.40 | 2.80 | 8.20 | 40.60 | 1.80 | 1.80 | 23.20 | 12.60 | 0.80 | 1.80 | 0.00 |
| >1.8g/cm$^3$ | 2.40 | 0.80 | 0.60 | 9.00 | 0.60 | 1.00 | 19.80 | 47.60 | 6.20 | 8.00 | 4.00 |

**Note:** RSF = reactive semi-fusinite, ISF = inert semi-fusinite, Fus/scl = fusinite & sclerotinite
Mic= micrinite, Inertodet = reactive and inert inertodetrinite, Total reactive macerals = vitrinite+liptinite+RSF

**Table 5.10:** Particle type analysis (microlithotype group analysis) on coal samples (%vol)

| Density fraction | Vitrite | Intermed | SF/Fus | Indet | Saprop -elic | Carb-argilite | Carb-ankerite | Carbopy rite | Minerals >60% |
|---|---|---|---|---|---|---|---|---|---|
| <1.5g/cm$^3$ | 23.80 | 20.60 | 45.80 | 7.80 | 0.40 | 0.80 | 0.60 | 0.40 | 0.00 |
| 1.5-1.8g/cm$^3$ | 1.60 | 6.60 | 50.20 | 26.60 | 0.80 | 7.20 | 5.60 | 1.00 | 0.40 |
| >1.8g/cm$^3$ | 1.40 | 1.00 | 7.20 | 11.20 | 0.00 | 18.60 | 5.20 | 8.80 | 46.6 |

**Note**: Intermed = mixed coal particles vitrinite, inertite and liptite
SF/fus = semi-fusite+fusite, Indet = inertodetrite, Sapropelic = liptinite rich particles
Carbominerite = organic and inorganic mineral matter associations, Carbargilite = coal + 20-60% clays/quartz included, Carbankerite = coal 20-60% carbonate minerals included, Carbopyrite = coal 5-20% pyrite included

### 5.3.2 Chemical analysis of density fractions

The ultimate and proximate results for the density coal fractions obtained from Coal and Mineral Technologies are summarized in Tables 5.11 and 5.12. The ultimate analysis of the float fraction shows that this fraction contains significant concentrations of C, H and S as compared with the sink fraction. As expected, the float fraction contains a lower ash content of 9.1% and significantly higher proportion of volatile matter, whilst the sink fraction contains a substantially higher ash content of 62.60% and a low content of volatile matter.

**Table 5.11**: Ultimate analysis of density coal fractions (dry, ash-free basis)

| Coal density Fractions | Carbon (%) | Hydrogen (%) | Nitrogen (%) | Total Sulphur (%) | Oxygen (%) |
|---|---|---|---|---|---|
| <1.5g/cm$^3$ | 78.25 | 4.33 | 2.05 | 0.68 | 14.69 |
| >1.5-1.8 g/cm$^3$ | 75.87 | 3.49 | 1.95 | 0.70 | 17.99 |
| >1.8g/cm$^3$ | 63.28 | 3.39 | 1.69 | 6.21 | 25.42 |

**Table 5.12:** Proximate analysis of feed coal and density coal fractions

| Coal density fractions | IM % | Ash % | VM % | FC % |
|---|---|---|---|---|
| Float ( <1.5g/cm$^3$) | 3.40 | 9.10 | 28.70 | 58.80 |
| Middling (>1.5-1.8 g/cm$^3$) | 4.60 | 23.70 | 21.90 | 49.8 |
| Sink (>1.8g/cm$^3$) | 2.00 | 62.60 | 16.70 | 18.70 |

**Note:** IM ……Inherent moisture
VM …..Volatile matter
FC……Fixed carbon

From the results given in Tables 5.13 and 5.14, it is clear that there is a general increase in the proportion of $SiO_2$, $Fe_2O_3$ and $K_2O$ with an increase in density and mineral matter proportions. In contrast, there is a general decrease in the proportion of $Al_2O_3$, $TiO_2$, $P_2O_5$, CaO, MgO and $Na_2O$ with an increase in density and mineral proportions (Table 5.13). These trends emphasize that $SiO_2$, $Fe_2O_3$ and $K_2O$ have a strong mineral affinity; whereas $Al_2O_3$, $TiO_2$, $P_2O_5$, CaO, MgO and $Na_2O$ have a strong carbon/organic affinity, either as included minerals and/or organically-bound inorganic elements. This could imply that these elements may interact differently at elevated temperatures during coal gasification or combustion.

**Table 5.13:** XRF analysis of the feed coal and density coal fractions (wt%)

| Sample number | Float <1.5 g/cm$^3$ | Middling >1.5-1.8 g/cm$^3$ | Sink >1.8g/cm$^3$ |
|---|---|---|---|
| $SiO_2$ | 44.20 | 50.40 | 56.70 |
| $Al_2O_3$ | 30.90 | 29.50 | 21.40 |
| $Fe_2O_3$ | 2.40 | 2.00 | 5.70 |
| $TiO_2$ | 2.20 | 1.50 | 1.10 |
| $P_2O_5$ | 1.50 | 1.00 | 0.40 |
| CaO | 8.60 | 7.90 | 6.80 |
| MgO | 3.10 | 2.80 | 1.30 |
| $K_2O$ | 0.70 | 0.70 | 0.90 |
| $SO_3$ | 5.70 | 4.20 | 7.00 |
| $Na_2O$ | 1.00 | 0.50 | 0.30 |
| **Total** | 100.00 | 100.00 | 100.00 |

### 5.3.3 Mineralogical analyses of float, middling and sink fractions from feed coal

Data on the different size and density fractions, also summarised in Table 4.11, indicate that the float fractions, with low percentages of LTA, have a mineral assemblage with lesser proportions of quartz and pyrite than the LTA-rich sinks fractions. Dolomite, by contrast, is more abundant in the floats and middlings fractions than in the high-density sinks material. This, together with the greater abundance of dolomite in the fine fractions than the coarse fractions, confirms a relatively intimate association of the carbonate minerals with the maceral components (in line with Table 5.8). Apart from a greater abundance of illite in the coarse floats material, the clay minerals, the phosphates and the bassanite, all appear to be more or less evenly distributed among the different size and density fractions.

- **CCSEM analysis of the float, middling and sink fractions**

The BSE images (Figure 5.4) of coal particles from the float, middling and sink fractions clearly show the substantial differences between these three density coal fractions. As before, in these back-scattered electron images, the appearance of carbon is black to dark grey and that of mineral matter is light grey to white.

Interestingly, the CCSEM analysis using BSE has successfully distinguished a “black” carbon phase and a “grey” carbon phase (Figure 5.4). This is specifically noted in the <1.5g/cm$^3$

density fraction. It is therefore proposed that this grey level discrimination is attributed to the variation in the density of macerals, ranging from 1.25g/cm$^3$ for liptinite, 1.3g/cm$^3$ for vitrinite and 1.5g/cm$^3$ for inertinite. Each density fraction has distinct particle characteristics (Figure 5.4). This illustrates the efficiency of density separation used in this study to produce float and sink fractions from the feed coal.

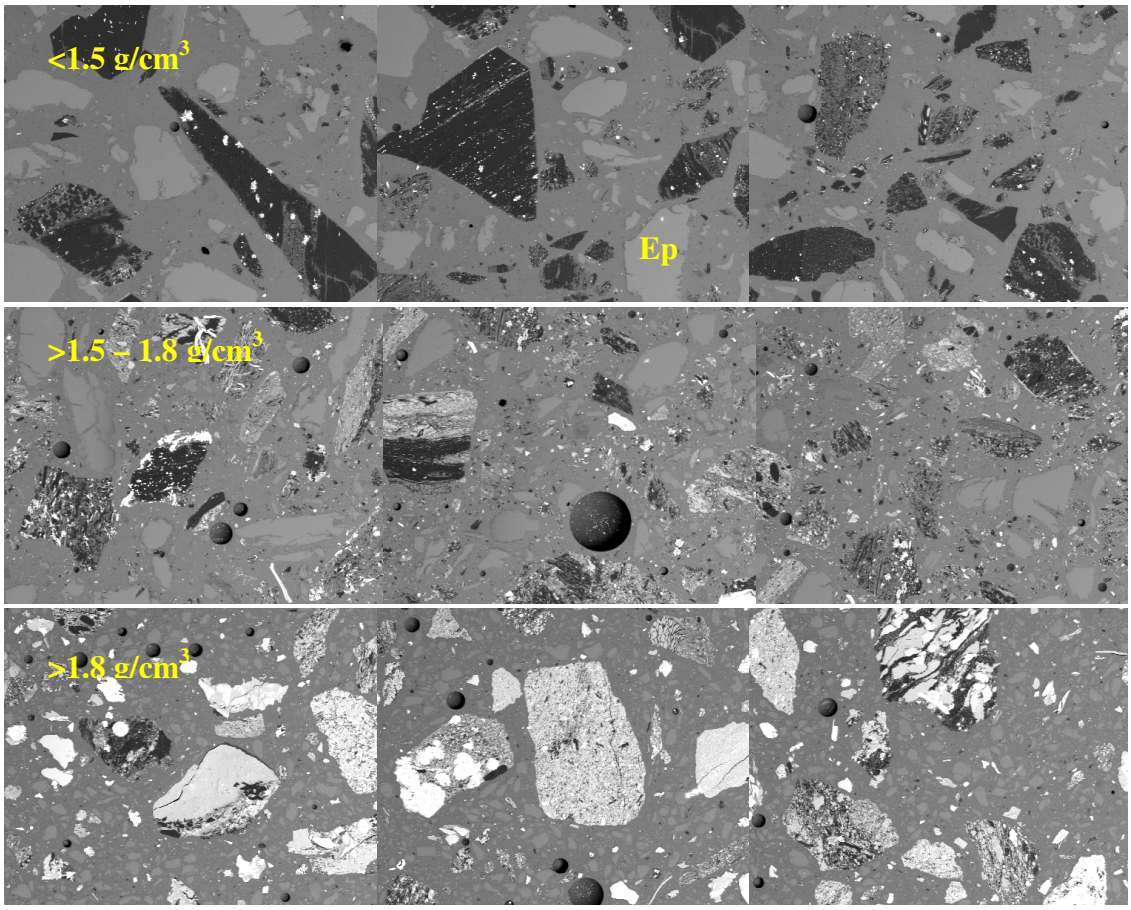


**Figure 5.4**: Back-scattered electron image of the three density fractions. The particle characteristics and variation in proportions of minerals are depicted. The width of each image is approximately 6.3mm. The large light grey particles (Ep) are included crushed iodinated epoxy resin particles.

- **Proportions of minerals present in the density coal fractions**

The mass-% mineral distribution as reported by CCSEM for the individual density fractions and the calculated total sample is summarised in Table 5.14. The concentration of the individual minerals present in Table 5.14, as well as the mass of the density fraction given in Table 3.1 were used to calculate the percent mineral distribution across the density coal fractions.

From Table 5.14 is clear that the proportions of minerals, with the exception of apatite, ankerite or siderite increases with an increase in density of the coal fractions. As expected, the ash yield of these density coal fractions increase. As expected, the organic fraction (macerals) significantly decreases with an increase in density of the coal fraction.

**Table 5.14**: Proportions of minerals in the float and sink fractions determined by CCSEM (mass percentage)

| Mineral | Idealised formula | Float fraction <1.5 g/cm$^3$ | Middling >1.5 - 1.8 g/cm$^3$ | Sink Fraction >1.8g/cm$^3$ |
|---|---|---|---|---|
| Pyrite | $FeS_2$ | 0.60 | 1.40 | 5.40 |
| Quartz | $SiO_2$ | 1.30 | 3.60 | 19.20 |
| Feldspar (Microcline) | $KAlSi_3O_8$ | 0.00 | 0.20 | 2.30 |
| Muscovite/illite | $K_2O.3Al_2O_3.6SiO_2.2H_2O$/ $K_{1.5}Al_4(Si_{6.5}Al_{1.5})O_{20}(OH)_4$ | 0.40 | 2.20 | 4.30 |
| Kaolinite | $Al_2Si_2O_5(OH)_4$ | 5.10 | 22.30 | 33.00 |
| Anatase/rutile | $TiO_2$ | 0.10 | 0.20 | 0.30 |
| Iron oxide/siderite | $Fe_2O_3/FeCO_3$ | 0.00 | 0.00 | 0.10 |
| Calcite | $CaCO_3$ | 0.90 | 1.80 | 7.80 |
| Dolomite | $CaMg(CO_3)_2$ | 1.50 | 4.00 | 3.10 |
| Ankerite | $(Fe, Ca, Mg)CO_3$ | 0.00 | 0.10 | 0.10 |
| Apatite | $Ca_5F(PO_4)_3$ | 0.20 | 0.20 | 0.10 |
| Other | Unidentified minerals | 0.30 | 1.30 | 0.60 |
| #Coal | Organic fraction | 89.50 | 62.70 | 23.70 |
| Total | | 100.00 | 100.00 | 100.00 |

**Note:** #Coal = refers the carbon-rich matrix and represents the macerals

Figure 5.5 shows the percent mineral distribution as function of density. Based on the results given in Figure 5.5, it is clear that high proportions of fluxing elements-bearing minerals (pyrite and calcite), with the exception of dolomite, report to the sink fraction (>1.8g/cm$^3$). Dolomite, which is the alternative source of the fluxing elements such as Ca and Mg, concentrated in the middling fraction (1.5-1.8g/cm$^3$ density fraction). This trend is attributed to significantly higher proportions of pyrite and calcite that occur as extraneous particles in the coal. However, a higher proportion of dolomite occurs as finer cleats between carbon-rich particles present in the middling coal fraction (1.5-1.8g/cm$^3$ density fraction). The high proportion of pyrite in the >1.8g/cm$^3$ density fraction is in line with the XRF analysis given in Table 5.13, showing a higher Fe content of this density fraction.

The >1.8g/cm$^3$ density fraction contains a significantly higher proportion of quartz, which is from rock fragments such as coarse to fine-grained arkosic sandstone. High concentrations of microcline/feldspars are contained in the >1.8g/cm$^3$ density fraction. As expected, kaolinite and muscovite/illite occur as fine included grains in the carbon matrix and are concentrated in the inertinite-rich particles (1.5-1.8g/cm$^3$ density fractions). In addition, a significant proportion of apatite is associated with the inertinite-rich particles (1.5-1.8g/cm$^3$ density fraction) and to a lesser extent with vitrinite-rich particles (<1.5g/cm$^3$ density fraction). Some preliminary results for the float and sink fractions found in this study are in line with previous results for density fractions of other South African coals that were found by Snyman et al. (1983).

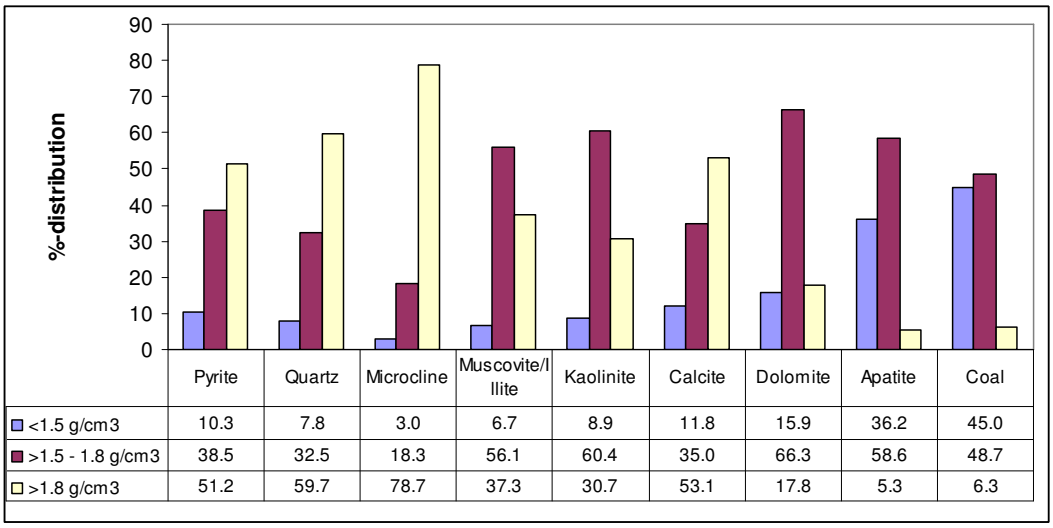


| | Pyrite | Quartz | Microcline | Muscovite/Illite | Kaolinite | Calcite | Dolomite | Apatite | Coal |
|---|---|---|---|---|---|---|---|---|---|
| <1.5 g/cm3 | 10.3 | 7.8 | 3.0 | 6.7 | 8.9 | 11.8 | 15.9 | 36.2 | 45.0 |
| >1.5 - 1.8 g/cm3 | 38.5 | 32.5 | 18.3 | 56.1 | 60.4 | 35.0 | 66.3 | 58.6 | 48.7 |
| >1.8 g/cm3 | 51.2 | 59.7 | 78.7 | 37.3 | 30.7 | 53.1 | 17.8 | 5.3 | 6.3 |

**Figure 5.5:** Mass % distribution of minerals in the density fractions.